Institute for Clinical and Experimental Surgery

Saarland University, Homburg/Saar, Germany

(Director: Prof. Dr. med. M. Laschke)

Pre-existing endometriotic lesions promote the development of new lesions in the abdomen of mice

Thesis

for acquiring the title of Doctor of Medicine at the Faculty of Medicine of Saarland University, Homburg

2025

Submitted by

Ilinca-Teodora Mihai

Born 10.06.1999 in Bucharest

TABLE OF CONTENTS

ABBREVIATIONS

3D	three-dimensional
AEC	3-amino-9-ethylcarbazole
ANOVA	analysis of variance
BL	bioluminescence
BLC	B-lymphocyte chemoattractant
C5/C5a	complement component-5a
CA-125	cancer antigen-125
CAG	chicken beta-actin/rabbit beta-globin
CD	cluster of differentiation
d	days
DNA	deoxyribonucleic acid
DMEM	Dulbecco's modified Eagle medium
DT	delayed transplantation
FACS	fluorescence-activated cell sorting
FITC	fluorescein isothiocyanate
G-CSF	granulocyte colony-stimulating factor
GFP	green fluorescent protein
GnRH	gonadotropin-releasing hormone
HE	hematoxylin and eosin
ICAM-1	intercellular adhesion molecule-1
IFN-gamma	interferon-gamma
IgG	immunoglobulin G
IHC	immunohistochemistry
IL	interleukin
Inc.	incorporated
IP-10	interferon gamma-induced protein-10
I-TAC	interferon-inducible T-cell alpha chemoattractant
JNKs	c-Jun N-terminal kinases
KC	keratinocyte chemoattractant
L^+	luciferase-positive

MCP-5	monocyte chemotactic protein-5
M-CSF	macrophage colony-stimulating factor
MIG	monokine induced by IFN-gamma
MIP-1a/2	macrophage inflammatory protein-1-alpha/2
MPO	myeloperoxidase
MRI	magnetic resonance imaging
NSAIDs	non-steroidal anti-inflammatory drugs
PBS	phosphate-buffered saline
PE	phycoerythrin
®	registered
rASRM	revised American Society for Reproductive Medicine
RANTES	regulated upon activation, normal T-cell expressed and presumably secreted
ROI	region of interest
SDF-1	stromal cell-derived factor-1
SEM	standard error of the mean
ST	simultaneous transplantation
TARC	thymus- and activation-regulated chemokine
TIMP-1	tissue inhibitor of metalloproteinases-1
™	trademark
TNF-α	tumor necrosis factor-α
TREM-1	triggering receptor expressed on myeloid cells-1
US	ultrasound
USA	United States of America
UTI	urinary tract infection
VEGF	vascular endothelial growth factor
WT	wild-type

1. SUMMARY

Endometriosis is a gynecological disease, which is defined by the development of endometriotic lesions outside the uterine cavity. Up to 20% of women of reproductive age are affected and show symptoms like dysmenorrhea, dyspareunia and infertility. This markedly reduces their quality of life. The reliable diagnosis of the disease can only be confirmed by laparoscopic surgery and histopathological analysis of tissue samples. Hence, several years can pass until patients are diagnosed correctly. The development of endometriosis is widely believed to be promoted by the process of retrograde menstruation according to the implantation theory of Sampson. This theory suggests that endometrial tissue fragments are transported to the abdominal cavity through the fallopian tubes and attach to the peritoneum, where they finally develop into endometriotic lesions. These lesions have been shown to change the peritoneal micromilieu.

This thesis analyzed if the presence of pre-existing endometriotic lesions supports the growth of new lesions. It also investigated if this is caused by an altered peritoneal environment or by an exchange of cells between individual lesions.

To test this, uterine tissue samples from FVB/N wild-type donor mice were transplanted simultaneously or time-delayed by 14 days with samples from transgenic FVB-Tg(CAG-luc-GFP)L2G85Chco/J donor mice into the abdomen of FVB/N wild-type recipient mice. The development of the lesions was monitored by using high-resolution ultrasound, bioluminescence imaging, histology and immunohistochemistry. Next, a peritoneal lavage was performed in additional FVB/N wild-type recipient mice in order to examine the peritoneal conditions after the induction of endometriotic lesions. For this, uterine tissue samples from transgenic FVB-Tg(CAG-luc-GFP)L2G85Chco/J donor mice were transplanted into the abdomen of recipient mice and peritoneal lavages were performed before and 14 days after transplantation. Flow cytometry and a cytokine array were used to assess the fraction of immune cells and levels of inflammatory cytokines in the peritoneal fluid.

The performed analyses showed that the growth of newly developing endometriotic lesions is promoted by the intraperitoneal presence of pre-existing ones. In fact, the time-delayed transplantation of uterine tissue samples resulted in higher growth rates of newly developing endometriotic lesions when compared to simultaneous transplantation. However, this cannot be explained by a cellular exchange between both lesion types (luciferase-positive lesions derived from FVB-Tg(CAG-luc-GFP)L2G85Chco/J mice and luciferase-negative lesions

derived from FVB/N wild-type mice), because no bioluminescent signals could be detected outside the luciferase-positive lesions. Therefore, this observation was rather caused by peritoneal inflammation, which was induced by the pre-existing lesions.

In line with this view, the analysis of peritoneal fluid after the induction of endometriotic lesions showed increased levels of several cytokines, such as B-lymphocyte chemoattractant (BLC), tissue inhibitor of metalloproteinases 1 (TIMP-1), interleukin (IL)-5 and IL-23, when compared to baseline conditions (before the induction of endometriotic lesions). Additionally, the performed flow cytometry showed a high fraction of Gr1-positive granulocytes in the peritoneal fluid after 14 days since the induction of endometriotic lesions.

These findings indicate that, in addition to other pathomechanisms, the development of endometriosis is driven by a lesion-induced peritoneal inflammation, which creates favorable conditions for the growth of new lesions.

2. ZUSAMMENFASSUNG

Die Endometriose ist eine gynäkologische Erkrankung, die durch die Entstehung von Endometrioseherden außerhalb der Uterushöhle gekennzeichnet ist. Bis zu 20% der Frauen im gebärfähigen Alter sind davon betroffen und zeigen Symptome wie Dysmenorrhoe, Dyspareunie und Infertilität. Dies beeinträchtigt ihre Lebensqualität deutlich. Die sichere Diagnose der Krankheit kann nur durch einen invasiven laparoskopischen Eingriff und eine histopathologische Untersuchung von Gewebeproben gestellt werden. Daher können mehrere Jahre vergehen, bis die Patientinnen die richtige Diagnose erhalten. Es wird allgemein angenommen, dass die Entstehung einer Endometriose durch retrograde Menstruation gemäß der Implantationstheorie von Sampson gefördert wird. Diese Theorie besagt, dass Fragmente von Endometriumgewebe durch die Eileiter in die Bauchhöhle transportiert werden und sich am Bauchfell festsetzen, wo sie sich schließlich zu Endometrioseherden entwickeln. Es wurde somit gezeigt, dass die Herde das peritoneale Mikromilieu verändern.

In der vorliegenden Arbeit wurde untersucht, ob bereits bestehende Endometrioseherde das Wachstum neuer Herde fördern. Außerdem wurde überprüft, ob dies auf ein verändertes peritoneales Milieu oder auf einen Zellaustausch zwischen einzelnen Herden zurückzuführen ist.

Zu diesem Zweck wurden Uterusgewebeproben von FVB/N-Wildtyp-Spendermäusen gleichzeitig oder um 14 Tage zeitversetzt mit Proben von transgenen FVB-Tg(CAG-luc-GFP)L2G85Chco/J-Spendermäusen in die Bauchhöhle von FVB/N-Wildtyp-Empfängermäusen transplantiert. Die Entwicklung der Herde wurde mittels hochauflösendem Ultraschall, Biolumineszenz-Bildgebung, Histologie und Immunhistochemie analysiert. Darüber hinaus wurde bei weiteren FVB/N-Wildtyp-Empfängermäusen eine Peritoneallavage durchgeführt, um die peritonealen Bedingungen nach der Induktion von Endometrioseherden zu untersuchen. Dazu wurden Uterusgewebeproben von transgenen FVB-Tg(CAG-luc-GFP)L2G85Chco/J Spendermäusen in die Bauchhöhle der Empfängertiere transplantiert und Peritoneallavagen vor und 14 Tage nach der Transplantation durchgeführt. Um den Anteil von Immunzellen und Entzündungsmediatoren in der Peritonealflüssigkeit zu bestimmen, erfolgte eine Durchflusszytometrie und ein Zytokin-Array.

Diese Untersuchungen zeigten, dass das Wachstum neuer Endometrioseherde durch das intraperitoneale Vorhandensein bereits bestehender Herde gefördert wird. Tatsächlich führte die zeitlich verzögerte Transplantation von Uterusgewebeproben zu höheren

Wachstumsraten von sich neu entwickelnden Endometrioseherden im Vergleich zur gleichzeitigen Transplantation. Dies konnte jedoch nicht durch einen Zellaustausch zwischen beiden Herdtypen (Luciferase-positive Herde aus FVB-Tg(CAG-luc-GFP)L2G85Chco/J-Gewebe und Luciferase-negative Herde aus FVB/N-Gewebe) erklärt werden, da außerhalb der Luciferase-positiven Herde keine Biolumineszenz-Signale nachgewiesen werden konnten. Daher war diese Beobachtung eher auf eine peritoneale Entzündung zurückzuführen, die durch die bereits bestehenden Herde ausgelöst wurde.

In Übereinstimmung damit zeigte die Analyse der Peritonealflüssigkeit nach der Induktion von Endometrioseherden erhöhte Konzentrationen von Zytokinen, wie B-Lymphozyten-Chemoattraktant (BLC), Gewebe-Inhibitor von Metalloproteinasen 1 (TIMP-1), Interleukin (IL)-5 und IL-23 im Vergleich zu den Ausgangsbedingungen (vor der Induktion von Endometrioseherden). Darüber hinaus zeigten durchflusszytometrische Analysen einen hohen Anteil an Gr1-positiven Granulozyten in der Peritonealflüssigkeit 14 Tage nach der Induktion von Endometrioseherden.

Diese Ergebnisse deuten darauf hin, dass die Entwicklung einer Endometriose neben anderen Pathomechanismen durch eine herdinduzierte peritoneale Entzündung vorangetrieben wird, die günstige Bedingungen für das Wachstum neuer Herde schafft.

3. INTRODUCTION

3.1. Endometriosis

3.1.1. Definition, symptoms and classification

Endometriosis is a chronic benign disease in gynecology with a high prevalence among young women. It is defined by the presence of ectopic endometrial glandular and stromal cells outside of the uterine cavity, leading to endometriotic lesions e.g. on the abdominal wall or peritoneal lining of intraabdominal organs. Affected patients suffer from symptoms such as dysmenorrhea, dyspareunia, dyschezia and infertility [Mounsey et al., 2006]. The patients' quality of life is markedly reduced due to frequent hospitalization, surgeries and disease recurrence rates of up to 80% [Gao et al., 2006; Ceccaroni et al., 2019]. Unfortunately, there is no reliable test or imaging available for the diagnosis of endometriosis other than an exploratory laparoscopy, a very invasive procedure for young women to undergo. More accessible methods of investigation, like ultrasound scans, are preferred to initially rule out gastrointestinal or reproductive pathologies that require immediate care (e.g. appendicitis, infections of the genital tract etc.). Due to such delays, many patients receive their correct diagnosis only 4-7 years after the onset of symptoms [Agarwal et al., 2019]. Consequently, the economic impact of the disease on the health care system must be considered as a relevant issue [Simoens et al., 2007; Surrey et al., 2020] along with the psychological impact on the affected patients, until they receive an appropriate treatment [Culley et al., 2013]. Therefore, more research in the field of endometriosis is urgently required.

Endometriotic lesions can be categorized into several types: superficial peritoneal endometriosis (located on the pelvic or abdominal peritoneum), ovarian endometrioma (ovarian cysts covered by an endometrial epithelium and frequently called "chocolate cysts") and deep-infiltrating endometriosis (a more invasive type of lesions, often affecting pelvic organs like the bowel, bladder or vagina) [Imperiale et al., 2023]. The three different types manifest differently and it has been suggested that they should be treated as separate entities with different pathogeneses [Nisolle & Donnez, 1997].

The classification of endometriosis is possible through multiple scoring systems. The most widely used is the revised American Society for Reproductive Medicine (rASRM) system due to its easy interpretation [Pašalić et al., 2023]. It divides endometriosis into four stages, based mainly on the size, location and amount of lesions. The stages ranging from I to IV, also

defined as “minimal”, “mild”, “moderate” and “severe disease”, correlate to the reached number of points at each case assessment. The size of the lesions mostly decides the attributed score (assigning points for < 1 cm, between 1-3 cm and > 3 cm lesion sizes). The disadvantage of this scoring system is its disregard of the infiltrating depth of the lesions. Another more descriptive system, the ENZIAN score, includes depth and localization assessment of endometriotic lesions [Tuttlies et al., 2005]. This classification system works by assigning a letter for the location of the lesions, followed by a number that describes the lesion size (e.g. P3: P for peritoneum, 3 for > 7 cm). Unfortunately, none of the mentioned scoring systems includes the severity of pain symptoms, which plays a significant role in the clinical manifestation of endometriosis and in deciding what treatment is indicated [Lee et al., 2021]. Additionally, both systems can only be used following a combination of imaging and surgical procedures. This has the purpose to guide clinicians towards further treatment and prognostic consultations.

3.1.2. Epidemiology

Approximately 16-20% of all women of reproductive age worldwide [Moradi et al., 2021] and 70% of those with chronic pelvic pain suffer from endometriosis [Parasar et al., 2017]. A population-based US study described an average incidence of 24.3 endometriosis cases per 10,000 person-years (a person-year is calculated by multiplying the number of study participants by the time each person spends in the study) [Christ et al., 2021]. Some known risk factors for developing endometriosis are early menarche, shorter menstrual cycle length and alcohol use. Infertility rates are relatively high in endometriosis patients, reaching up to 50% [Giudice & Kao, 2004]. Moreover, infertile women show a prevalence of endometriosis ranging from 20 to 50% [Practice Committee of the American Society for Reproductive Medicine, 2012]. Since the diagnosis of endometriosis often relies on performing a laparoscopy, but infertility alone is not an indication for it, the prevalence among infertile women may be even underestimated [Coccia et al., 2022].

It should also be noted that the true prevalence and incidence of the disease are difficult to assess, because meta-analysis studies often show certain variability in the diagnostic management of endometriosis [Sarria-Santamera et al., 2021]. This means that in some cases, diagnosis criteria for endometriosis patients aren’t based on the gold standard of laparoscopy [Hsu et al., 2010] and may rely only on clinical examinations or imaging, such as ultrasound or magnetic resonance imaging (MRI). The presence of asymptomatic endometriosis can also not be ruled out.

3.1.3. Diagnosis and treatment

Since most women with endometriosis show little to no abnormalities during physical examination, a preliminary diagnosis is often achieved based on their clinical history, like pain symptoms and menstrual cycle history. Nevertheless, the most common finding is a tenderness of the posterior vaginal fornix at palpation [Parasar et al., 2017], equivalent to discomfort at palpation of the Douglas pouch (also called rectouterine pouch). In this case, other causes for lower abdominal pain, such as adhesions, gastrointestinal or urological pathologies must be ruled out. A few examples are chronic inflammatory bowel diseases (like Crohn's disease), diverticulitis, urolithiasis (kidney stones), urinary tract infection (UTI) or adnexitis. In addition, an ectopic pregnancy should always be ruled out when examining young women with persistent abdominal pain. Therefore, diagnostic procedures such as urinalysis, pregnancy test, endocervical smear test and ultrasound are necessary.

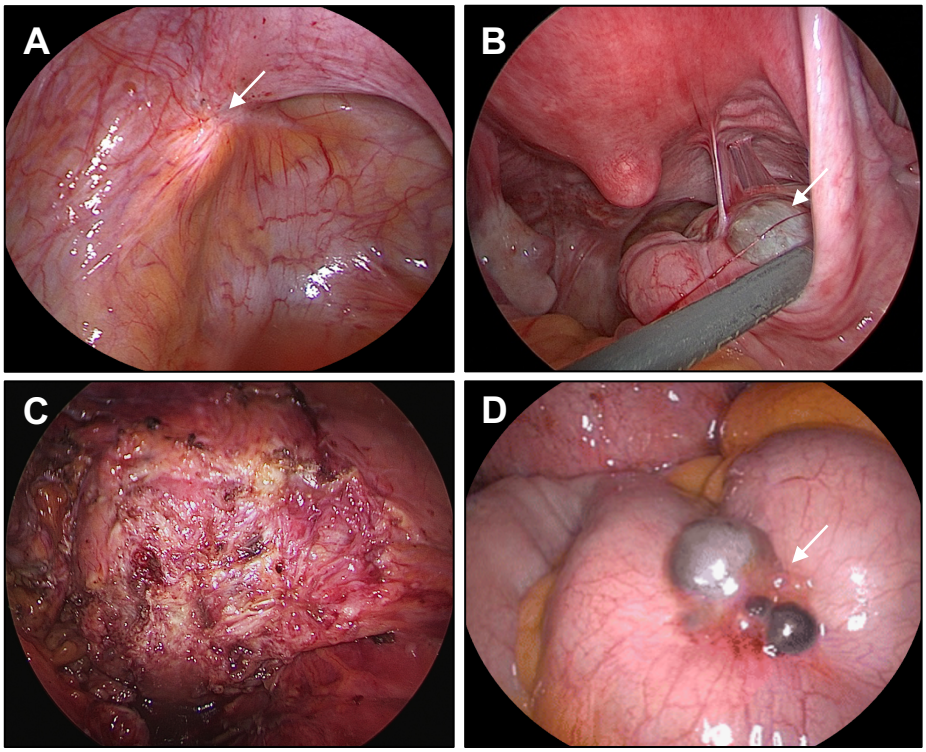

Figure 1. *Endometriotic lesions imaged during laparoscopy. (**A**) Superficial endometriotic lesion (arrow) on the pelvic peritoneum of the sacrouterine ligament. (**B**) Endometrioma of the left ovary (arrow), made visible by the use of a laparoscopy instrument. Adhesions are visible above the endometrioma. (**C**) Deep-infiltrating endometriosis on the rectum. (**D**) Endometriotic lesions (arrow) on the small intestine. [(**A**,**B**,**C**): adapted from Siegenthaler et al., 2020; (**D**): adapted from Al-Talib & Tulandi, 2010]*

The diagnostic gold standard for endometriosis is an exploratory laparoscopy [Hsu et al., 2010] (Figure 1). If suspicious lesions are discovered during this procedure, they can be excised and

histopathologically confirmed. Subsequently, the patient may be offered post-operative treatment [Becker et al., 2022]. However, current guidelines speak against performing a laparoscopy for the sole purpose of diagnosing endometriosis and rather recommend a focus on the clinical diagnosis based on symptoms and imaging [Allaire et al., 2023]. It has been shown that transvaginal ultrasound and MRI are reliable imaging techniques for the diagnosis of ovarian endometrioma and deep-infiltrating endometriosis [Nisenblat et al., 2016]. Ultrasound imaging is considered a first-line investigation for patients suspected of endometriosis and is widely available. Still, both ultrasound and MRI have been shown to be equally accurate for the diagnosis of endometrioma, replacing the exploratory laparoscopy. Transvaginal ultrasound examination was even better for the analysis of anatomical sites with deep-infiltrating endometriosis when compared to MRI, leading to a better planning of operative procedures [Nisenblat et al., 2016]. Unfortunately, superficial peritoneal endometriosis cannot be reliably detected by any of the mentioned imaging techniques. In this case, laparoscopy remains the best option for symptomatic patients suspected to exhibit peritoneal lesions [Allaire et al., 2023].

In search of easier and less invasive alternatives to a diagnostic laparoscopy, many research groups hoped to identify a specific endometriosis biomarker in either blood, urine or menstrual fluid. Several analyses showed altered levels of distinct biomarkers, such as vascular endothelial growth factor (VEGF) and cancer antigen (CA)-125, but none proved to be sufficiently reliable [May et al., 2011; Vodolazkaia et al., 2012].

The clinical management of endometriosis implies surgical, hormonal and pain therapy. First-line pain management is achieved by non-steroidal anti-inflammatory drugs (NSAIDs) to reduce symptoms of dysmenorrhea and any other endometriosis-associated pain [Becker et al., 2022]. Additionally, patients should be offered hormonal therapy, such as combined oral contraceptive pills (ethinyl estradiol and progestins) or progestin-only contraceptives [Zito et al., 2014]. These have been shown to significantly reduce dysmenorrhea, dyspareunia as well as non-cyclical pelvic pain with an overall improvement of the quality of life [Grandi et al., 2019]. An alternative to the mentioned medication is second-line gonadotropin-releasing hormone (GnRH) agonists or GnRH antagonists, since the standard oral contraceptive therapy proved to be effective for only two-thirds of patients experiencing endometriosis-associated pain. Both GnRH-modulating medications induce a hypoestrogenic state and cause anovulation and amenorrhea, hereby effectively reducing pelvic discomfort in endometriosis patients when following long-term treatment [Resta et al, 2023]. Administration should be limited to 6 months for GnRH agonists and to 24 months for GnRH antagonists due

to their induced hypoestrogenic side effects, such as a loss of bone mineral density and vasomotor symptoms (i.e. hot flushes, headaches) [Surrey, 2022; Whitaker et al., 2022].

Surgical treatment includes the laparoscopic excision of endometriotic lesions and any irreversibly affected parts of organs (e.g. parts of the rectum or the bladder in rare severe cases of deep-infiltrating endometriosis). Studies showed that the excision of endometriotic lesions is superior to ablation, significantly improving pain symptoms 12 months post-surgery [Pundir et al., 2017]. Moreover, successful surgeries also increase the postoperative spontaneous pregnancy rates in patients with infertility associated with endometriosis [Jacobson et al., 2010].

3.2. Pathogenic mechanisms and their investigation

3.2.1. Etiology

A possible explanation for the development of endometriosis is the implantation theory of Sampson [1927]. This theory states that, during menstruation, vital endometrial cells are shed retrogradely from the uterus through the fallopian tubes and implant themselves onto the peritoneum of the abdominal cavity. There, they can develop into vascularized endometriotic lesions (Figure 2). Since Sampson's postulate, clinical advances have been progressively made, which provided several scientific proofs on a molecular and cellular level for this long-established theory. A study of Bulun [2022] could show that endometriotic cells (from ovarian endometriomas, deep-infiltrating or superficial lesions) and intracavitary endometrial cells share common DNA patterns. These consisted of several somatic mutations in clusters of endometrial epithelial cells (found in the uterine lining), which were identical to the mutations found in endometriotic lesions. A similar finding was reported for endometriotic stromal cells (in endometriotic lesions), which harbored epigenetic defects, leading to an elevated synthesis and secretion of cytokines and chemokines. The same defects were then found in endometrial stroma cells (stroma cells of the uterine lining), only less pronounced [Bulun et al., 2019]. The discovery of matching genetic defects in the eutopic endometrium and endometriotic lesions of patients supports the theory that endometriosis originates from retrograde menstruation. Other studies showed that the eutopic endometrium (in the uterus) is different from healthy controls in individuals with endometriosis [Liu & Lang, 2011; Brosens et al., 2012]. This may lead to new insights for diagnosis and treatment management of endometriosis in the future.

There are also other theories for the development of endometriosis, such as hematogenous or lymphatic spreading of endometrial cells, metaplasia or stem cell recruitment [Signorile et al., 2022]. The metaplasia theory stated by Gruenwald [1942] considers an embryological relation between celomic walls (peritoneal serosa) and the Mullerian ducts (the embryological origin of the female reproductive tract), therefore leading to metaplastic cell differentiation into endometriosis at peritoneal sites. As support to this theory, a published case report in 2010 described a 20-year-old patient with Mayer-Rokitansky-Küster-Hauser syndrome, which is a rare congenital reproductive disorder in females, where both the uterus and vagina are underdeveloped or nonexistent. The patient suffered from chronically increasing pelvic pain and eventually underwent laparoscopy. Agenesis of the uterus, vagina and fallopian tubes was confirmed and minimal (small, superficial) endometriotic lesions were identified and excised. Another laparoscopic surgery was performed 5 years later due to recurrent endometriosis [Mok-Lin et al., 2010].

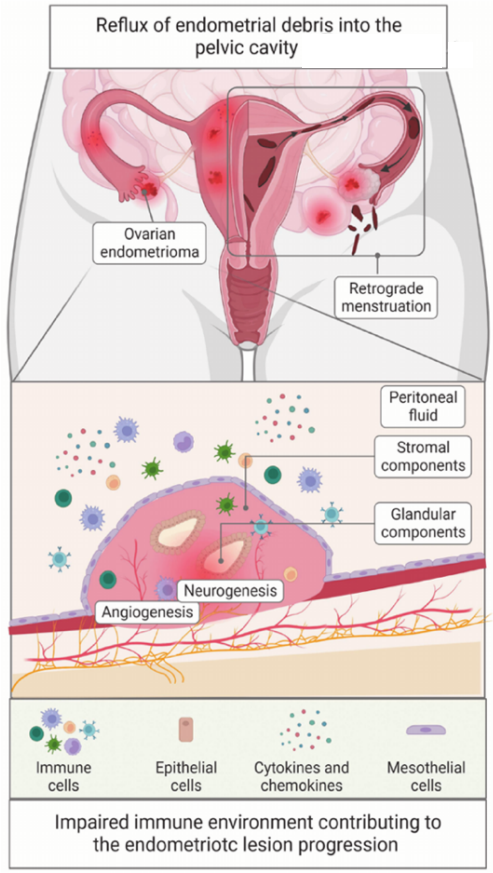

Figure 2. *The development of endometriosis according to Sampson's retrograde menstruation theory: stromal and glandular debris tissue is shed into the pelvic cavity, which triggers an aberrant immune reaction of the cellular micromilieu in the peritoneal fluid. This leads to induction of inflammation, angiogenesis and neurogenesis, supporting endometriotic lesion progression. Lesions are shown on the uterus (superficial endometriosis), ovary (endometrioma) and on the colon (deep-infiltrating endometriosis). [Adapted from Fan et al., 2023]*

The stem cell recruitment theory states that stem cells originating from the bone marrow or eutopic endometrium migrate into soft tissues outside of the uterus [Tampaki et al., 2017]. They may then differentiate into endometrial stroma or glandular cells. However, this cellular misplacement mechanism includes the other theories, like retrograde menstruation and hematogenous or lymphatic metastasis. By this, the stem/progenitor cells are relocated and establish ectopic endometriotic lesions. Additionally, these stem cells must coordinately differentiate into multiple cellular components, like stroma, glands and smooth muscle cells. This involves a complex series of pathophysiological mechanisms that are not yet completely elucidated [Maruyama, 2022].

Further theories have been formulated for the origin of ovarian endometrioma. One of them states that adhesions formed between the ovary and the peritoneum facilitate the implantation of endometriotic implants transported via retrograde menstruation. Next, the ovarian cortex (outer layer) invaginates around the attached implant, which actively bleeds and therefore leads to the formation of an ovarian cyst [Imperiale et al., 2023].

The pathogenesis of deep-infiltrating endometriosis has also been studied, describing a different behavior than ovarian and peritoneal endometriosis. Histological analyses showed that deep-infiltrating lesions contain a large number of undifferentiated glandular cells. These have a higher tissue resistance to the immunosuppressive effects of the peritoneal fluid, leading to the ability of the lesions to infiltrate deeper into the surrounding tissue [Abrao et al., 2003; Tosti et al., 2015].

3.2.2. The peritoneal environment

The presence of endometriosis is known to alter the physiological microenvironment of the peritoneal cavity, which leads to inflammation and angiogenesis through various cytokines and growth factors in the peritoneal fluid [Rakhila et al., 2016; Jorgensen et al., 2017]. Although no single cytokine or marker has been found specific for endometriosis, previous comparisons between peritoneal fluid from women with and without endometriosis have shown marked differences in profiles of measured cytokines [Kalu et al., 2007]. Elevated cytokines in the peritoneal fluid of women with endometriosis are interleukin (IL)-1, IL-5, IL-6, IL-8, IL-17, tumor necrosis factor (TNF)-α and VEGF [Harada et al., 2001]. The increased secretion of these factors is caused by an imbalance of immune cells in the peritoneal fluid. For instance, T-cell subtype levels vary in endometriosis. Hence, cytotoxic T-cells (cluster of differentiation (CD)8^+ cells) have been shown to exhibit a lower cytotoxicity against ectopic autologous endometrial cells [Schmitz et al., 2021]. Furthermore, T-helper-cells ($CD4^+$ cells)

of the Th17 type are significantly elevated in the peritoneal fluid of endometriosis patients compared to healthy women and the number of cells correlate with the severity of the disease [Gogacz et al., 2016]. IL-17, “the signature cytokine” derived from Th17 cells, is accordingly increased, contributing to the appearance, development and progression of endometriotic lesions [Fan et al., 2023].

Granulocytes are another type of immune cells that are involved in the pathophysiology of endometriosis. Neutrophilic granulocytes are one of the main secretors of VEGF in endometriotic lesions and, thus, support angiogenesis. The above-mentioned IL-17 also acts as a chemoattractant for neutrophils, and it was shown that these cells are increased in the peritoneal fluid of women with endometriosis. They also produce reactive oxygen species, which further promotes the progression of the disease [Vallvé-Juanico et al., 2019]. In line with this fact, a study in neutrophil-depleted mice showed a reduced formation of endometriotic lesions [Takamura et al., 2016].

Furthermore, the number of macrophages in peritoneal fluid has been shown to positively correlate with pain severity in patients with endometriosis [Morotti et al., 2014]. Macrophages secrete TNF-α, a cytokine that stimulates nerve growth factor and promotes the development and survival of nerve fibers. As expected, pelvic pain correlates with the density and hypertrophy of nerves in endometriotic lesions [Wu et al., 2017]. Macrophages also contribute to infertility in affected patients by compromising oocyte function through secretion of specific cytokines, such as c-Jun N-terminal kinases (JNKs) [Beste et al., 2014].

The above-mentioned roles of immune cells in the pathophysiology of endometriosis indicate that inflammation is a key factor for the development of endometriotic lesions in the peritoneal cavity. Accordingly, this thesis analyzed the impact of a lesion-induced inflammatory environment on the development of new endometriotic lesions.

3.2.3. Previous research

Endometriosis studies are often performed in rodents. The murine model shows similarities to humans in anatomical, physiological and genetic features [Bryda, 2013; Greaves et al., 2014], which makes it an appropriate substitute for human subjects in basic research or preclinical studies. However, mice are mammals which do not experience retrograde menstruation. Therefore, endometriosis must be induced iatrogenically in these animals. This can be achieved by transplantation of uterine tissue fragments into the abdomen of the animals [Körbel et al., 2010]. Once attached to the peritoneum, the fragments develop into

endometriotic lesions. The transplantation of uterine tissue into the abdominal cavity can be performed either surgically or by injection. This means that the tissue fragments can be sutured on desired sites of the peritoneum after the surgical opening of the abdomen (laparotomy) or intraperitoneally injected as a suspension [Burns et al., 2022]. For the experiments of the present thesis, the surgical transplantation technique was used.

A previous endometriosis study could demonstrate the ability of individual green fluorescent protein (GFP)-positive endometrial cells to integrate into pre-existing endometriotic lesions in mice [Tal et al., 2019]. In this study, endometriosis was induced in C57BL/6J female mice by suturing uterine tissue samples to the peritoneum. After one week, a suspension of GFP-expressing uterine cells (from minced uteri of GFP-expressing donors) was injected into the peritoneal cavity of the animals. Controls were injected with phosphate-buffered saline (PBS). After another three weeks, the lesions were excised and analyzed by flow cytometry and immunohistochemistry. This showed that individual GFP-positive cells were integrated in the newly developed endometriotic lesions, mainly as part of the stroma and walls of blood vessels. In summary, Tal's et al. model simulated retrograde menstruation by demonstrating the contribution of individual uterine cells found in the peritoneal fluid to the development of lesions. Therefore, the injected cell suspension mixed with the peritoneal fluid intraperitoneally imitated menstrual material shed into the abdominal cavity. The model illustrated the potential for continuous lesion development through individual cell integration, supported by retrograde menstruation [Tal et al., 2019]. As a further step, the present thesis aimed to examine whether peritoneal endometriotic lesions exchange cells with each other in a manner that sustains disease progression.

Sampson's retrograde menstruation theory may explain the chronic aspect of the disease due to the monthly shed endometrial cells into the peritoneal cavity and continuous development of new lesions [Sampson, 1927]. However, this alone does not account for the pathophysiology of the disease. Blood was found in the peritoneal fluid of most healthy menstruating women, up to 90% [Halme et al., 1984]. Thus, a susceptibility to develop endometriosis of certain individuals may be speculated, like an altered inflammatory cytokine profile. Jiang et al. [2021] showed that women with endometriosis have modified intestinal or reproductive tract microbiota when compared to healthy individuals. These patients were inclined to develop a chronic state of inflammation due to disrupted immune function in the abdominal cavity. The present thesis therefore also analyzed cytokines and growth factor levels in the peritoneal cavity of mice after endometriosis induction, aiming to illustrate the key role of inflammation in the development of endometriotic lesions.

In 1997, Nisolle and Donnez classified endometriotic lesions into three categories: red lesions (in an early developmental stage with a dense vascularization), black lesions (a result of inflammation and scarification processes) and white lesions (fibrotic and inactive) [Nisolle & Donnez, 1997]. This shows that there are stages of a lesion's life cycle and supports the idea of a continuously changing biological micromilieu undergoing inflammatory and angiogenic processes that are most likely triggered by the presence of lesions. Accordingly, the purpose of this thesis was to clarify whether the pre-existence of endometriotic lesions creates a favorable environment for the development and growth of new ones.

3.2.4. The endometriosis mouse model

The present thesis studied the development of endometriosis in a mouse model. The transplantation experiments were performed with donor mice, which were used for the isolation of uterine tissue samples, and recipient FVB/N wild-type mice, which received implanted tissue samples in their peritoneal cavity. Donor animals were chosen from two mouse strains: transgenic FVB- Tg(CAG-luc-GFP)L2G85Chco/J mice and FVB/N wild-type mice. The endometriotic lesions derived from the two distinct types of tissues could therefore be monitored for growth behavior and excised at the end of the experiments to undergo further processing.

In the used transgenic mouse line, all cells express firefly luciferase enhanced green fluorescence protein directed by the human cytomegalovirus immediate early promoter enhancer with chicken beta-actin/rabbit beta-globin hybrid (CAG) promoter. The transgenic mouse construct was designed by the laboratory of Dr. Christopher H. Contag (Stanford University School of Medicine) (https://www.jax.org/strain/008450). The tissue of the mice becomes luminescent when the expressed luciferase reacts with administered luciferin. This enables bioluminescence imaging to analyze the potential recruitment of luciferase-positive cells into lesions formed from luciferase-negative uterine tissue samples.

In addition, the growth, proliferation, vascularization and immune cell infiltration of newly developing endometriotic lesions were analyzed through high-resolution ultrasound, histology and immunohistochemistry. To examine the peritoneal environmental changes after the induction of endometriotic lesions, flow cytometry and a cytokine array assessed immune cells and inflammatory factors in the peritoneal fluid.

4. AIM OF THE STUDY

This thesis analyzed the effects of pre-existing endometriotic lesions in the peritoneal cavity on the growth of new ones. For this purpose, an endometriosis mouse model was used. Lesions were induced by means of surgical transplantation. In vivo monitoring was performed through high-resolution ultrasound examinations. Additionally, due to transplantation of luciferase-expressing uterine tissue samples in recipient mice, cell migration between individual lesions was monitored by means of bioluminescence imaging. The aim of the thesis was to test the following hypotheses:

1. Pre-existing endometriotic lesions in the peritoneal cavity promote the growth of new lesions through microenvironmental changes.
2. Individual endometriotic lesions exchange cells between each other, which promotes the progression of the disease.
3. Pre-existing endometriotic lesions in the peritoneal cavity provoke a local inflammatory response.

5. MATERIALS AND METHODS

5.1. Animals

In all experiments, 12- to 20-week-old female FVB/N wild-type mice and FVB-Tg(CAG-luc-GFP)L2G85Chco/J transgenic mice (Institute for Clinical and Experimental Surgery, Homburg, Germany) were used. These had an average bodyweight of 18-25 g. The mice were maintained in groups of two to four per cage. They were housed on wooden chip bedding with access to standard pellet food (Altromin, Lage, Germany) and water ad libitum. The mice were kept in the conventional animal facility of the Institute for Clinical and Experimental Surgery with a 12 h day-night cycle. All animals were regularly weighed and checked for signs of distress (poorly groomed fur, closed eyes, reduced activity, unusual behavior, hunched back) using internal standardized score sheets. Any stressed individuals were given 10 mg/kg Caprofen subcutaneously (Rimadyl®, Zoetis Germany GmbH, Germany) as pain medication and 1 mL 0.9% saline subcutaneously for volume substitution. Each recipient mouse included in the transplantation experiments was marked during anesthesia on its tail (with waterproof marker) and its ears (pierced) for easy animal identification.

All animal experiments were performed according to the German legislation on protection of animals and the National Institutes of Health Guide for the Care and Use of Laboratory Animals (Institute of Laboratory Animal Resources, National Research Council, Washington, DC, USA) and were approved by the local governmental animal protection committee (permission number: 38/2019).

5.2. Estrous cycle and vaginal lavage

Female mice are mammals which exhibit an estrous cycle of about 4 days with each phase of the cycle taking approximately one day. The first phase, proestrus, is characterized by the presence of parabasal nucleated epithelial cells and intermediary cells in vaginal smear samples (Figure 3A). As the phase of estrus begins, a majority of anucleated cornified epithelial cells can be seen (Figure 3B). The following metestrus phase shows a mix of cornified epithelial cells and leukocytes (Figure 3C), and the diestrus is typically associated with high leukocyte numbers (Figure 3D) [Cora et al., 2015; Pantier et al., 2019].

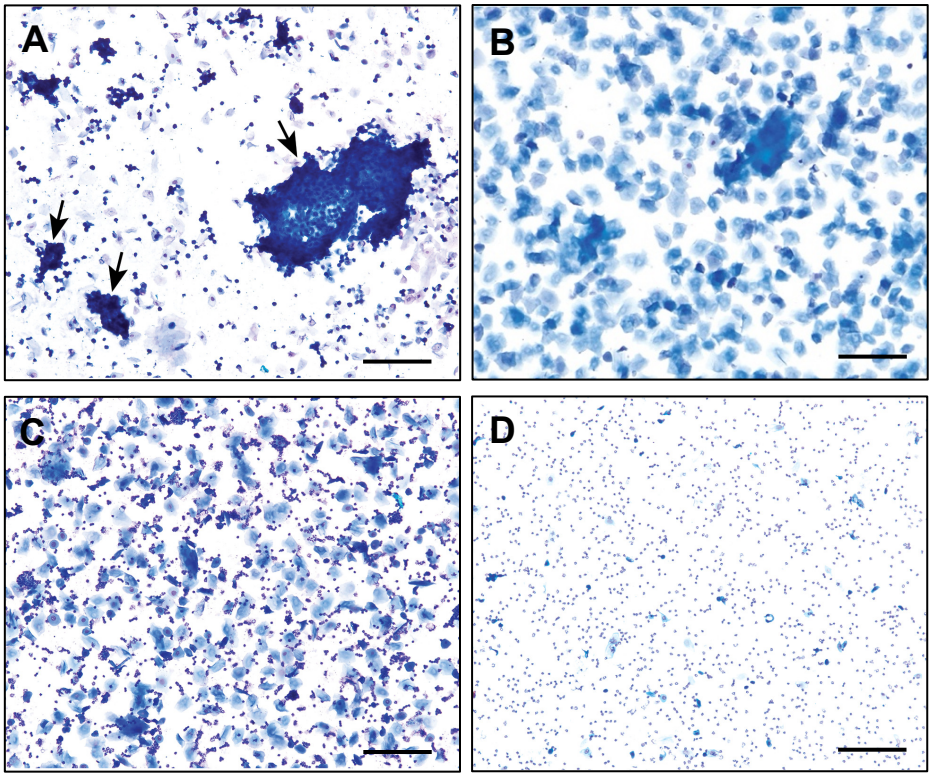

Figure 3. *Cellular characteristics of the estrous cycle. Modified Wright-Giemsa-stained vaginal smears from Sprague Dawley rats (**A**) and B6C3F1/N mice (**B**-**D**). (**A**) The proestrus is characterized by high numbers of small nucleated epithelial cells forming some scattered cohesive cell clusters (arrows). (**B**) The estrus presents with high numbers of anucleated epithelial cells. These appear larger, more evenly dispersed, and higher in numbers than proestrus nucleated cells. (**C**) The metestrus begins with the appearance of dispersed neutrophils among the anucleated epithelial cells. Cell numbers decrease as the rodent transitions into the diestrus. (**D**) The diestrus is characterized by predominantly neutrophils with low numbers of scattered epithelial cells. Scale bars: 300 µm. [Adapted from Cora et al., 2015]*

For the following experiments, vaginal lavage samples were analyzed cytologically to determine the estrous cycle stages, ensuring that all animals were in the identical stage. For this, a phase-contrast microscope (CH-2; Olympus; Hamburg, Germany) was used to examine cell suspensions obtained after carefully pipetting 15 µL of 0.9% saline into the vagina of the animals [Rudzitis-Auth et al., 2022a]. Both donor mice used for the isolation of uterine tissue samples as well as recipient mice for the induction of endometriotic lesions were chosen only if they were in the stage of estrus.

5.3. Isolation of uterine tissue samples from donor mice

To induce peritoneal endometriotic lesions, uterine tissue samples were excised from FVB/N wild-type and transgenic FVB-Tg(CAG-luc-GFP)L2G85Chco/J mice in the stage of estrus. For this purpose, the animals were anesthetized by administrating an intraperitoneal injection of

100 mg/kg ketamine (Ursotamin®; Serumwerke Bernburg, Bernburg, Germany) and 12 mg/kg xylazine (Rompun®; Bayer, Leverkusen, Germany). Once the paw withdrawal reflex was negative (an objective method to assess pain sensation in mice), the animals were fixated in supine position.

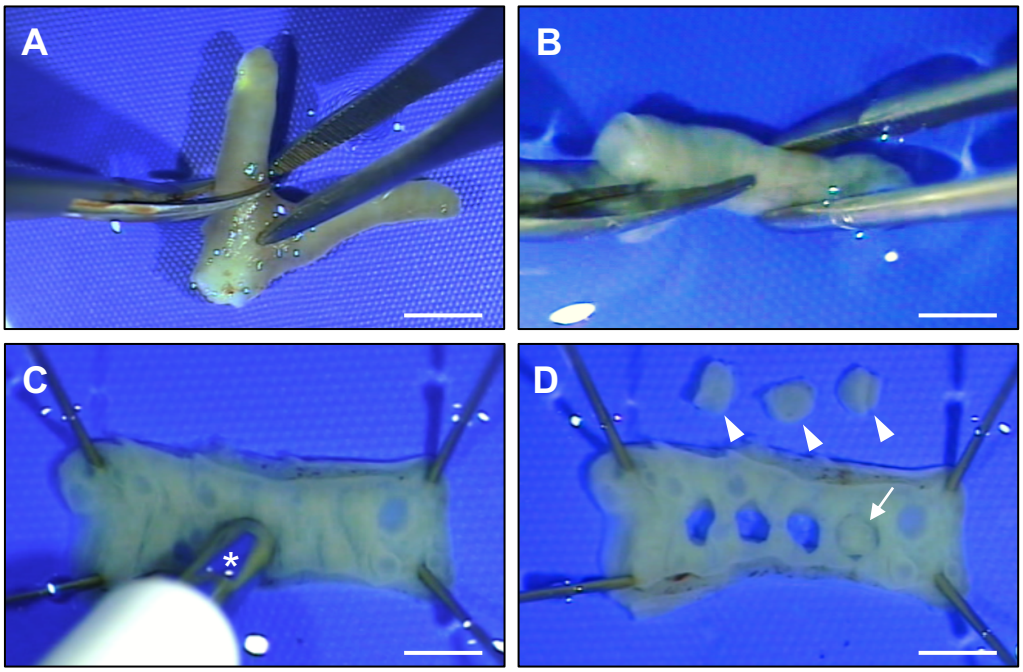

Figure 4. *Generation of uterine tissue samples. (**A**) Isolated bicornuated uterus cut at the cervical level and with adnexa removed. The uterine junction is held by fine anatomical forceps while the right uterine horn is cut by means of microscissors. Scale bar: (**A**) = 5 mm. (**B**) Longitudinal opening of the uterine horn with microscissors. (**C**) Longitudinally opened uterine horn with endometrial lining exposed and fixated by four cannulas (26G) in each corner. A dermal biopsy punch (∗) is pressed into the uterine lining for the excision of uterine tissue samples with a diameter of 2 mm (samples may appear smaller in images due to contraction of muscle fibers after excision). (**D**) Three excised uterine tissue samples (arrowheads) placed next to the upper side of the fixated uterine horn and one uterine tissue sample (arrow) directly after excision and prior to its removal from the uterine horn with fine forceps. Scale bars: (**B**,**C**,**D**) = 3 mm.*

The skin was disinfected and a midline laparotomy was performed with additional transversal incisions below the kidney level. The bowel was carefully moved outside the abdominal cavity, the uterus was identified for excision and transferred into a Petri dish containing Dulbecco's modified Eagle medium (DMEM; PAN Biotech, Aidenbach, Germany; 10% fetal calf serum, 100 U/mL penicillin, 0.1 mg/mL streptomycin (Thermo Fisher Scientific, Dreieich, Germany)). The uterine horns were isolated under a stereomicroscope (M651; Leica Microsystems GmbH, Wetzlar, Germany) (Figure 4A). The donor mice were then euthanized by incision of the inferior vena cava. The uterine horns were opened longitudinally (Figure 4B) and 2 mm tissue samples were excised by use of a dermal biopsy punch (Stiefel Laboratorium GmbH, Offenbach am Main, Germany) (Figures 4C-D).

5.4. Induction of endometriotic lesions in the abdominal cavity

In order to surgically induce endometriotic lesions, uterine tissue samples from transgenic and wild-type mice were transplanted into the abdomen of wild-type mice, as described before [Rudzitis-Auth et al., 2022b]. The anesthesia of mice was achieved by administrating an intraperitoneal injection of 100 mg/kg ketamine (Ursotamin®; Serumwerke Bernburg) and 12 mg/kg xylazine (Rompun®; Bayer). Subsequently, they were fixated in supine position, shaven and given eye cream to prevent dryness of the cornea. Surgery was performed on heated mats to prevent lowered body temperature during anesthesia. Following midline laparotomy (Figure 5A), the uterine tissue samples were fixated with 6-0 Seramon sutures (Serag-Wiessner Products, Naila, Germany) to the peritoneal wall. For this purpose, the suture needle was inserted through the center of the tissue sample on its endometrial side (Figure 5B) and then pierced through the abdominal peritoneum to generate a simple surgical knot.

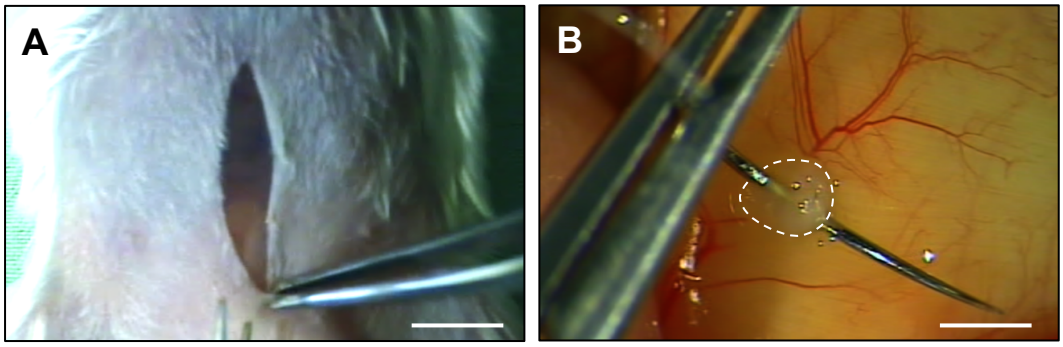

Figure 5. *Surgical induction of endometriotic lesions. (**A**) Median laparotomy of a shaven mouse with skin incision and peritoneum still intact. Forceps at inferior pole of the incision. Scale bar: (**A**) = 5 mm. (**B**) Uterine tissue sample (borders marked by broken line) fixed by a suture needle in a needle holder. The background shows the left abdominal peritoneum with blood vessels. Scale bar: (**B**) = 2 mm.*

Next, the laparotomy was closed with running 5-0 Prolene sutures (Ethicon Products, Norderstedt, Germany). All animals received postoperative care consisting of subcutaneously administered 1 mL 0.9% saline for volume substitution and 10 mg/kg Caprofen (Rimadyl®; Zoetis Germany GmbH) as pain medication for prevention of distress. Additionally, they were left to recover in their cages in front of infrared lamps to provide heat for a few hours.

5.5. High-resolution ultrasound imaging

A Vevo LAZR system (FUJIFILM VisualSonics Inc., Toronto, ON, Canada) equipped with a 256-element linear-array transducer (LZ 550; FUJIFILM VisualSonics Inc.) and set on a center frequency of 40 MHz was used for analyzing the development of induced endometriotic lesions. For this, the mice were anesthetized with 2% isoflurane in oxygen. To minimize distress provoked by handling, they were placed freely inside a transparent box with narcotic gas input and let to fall asleep (Figure 6). The mice were fixated in supine position on a heated stage with a gas mask for continuous inhalational anesthesia. Their abdomen was then chemically depilated for best imaging quality (Veet Hair Removal Cream; Reckitt Benckiser Germany, Heidelberg, Germany). By use of the Vevo imaging station (FUJIFILM VisualSonics Inc., Toronto, ON, Canada) equipped with a heated mouse platform (Figure 7A-B), the heart and respiratory rate were monitored while also maintaining a body temperature of 36-37 °C. The isoflurane gas concentration was reduced accordingly at any sign of anesthetic overdose (irregular breathing, bradypnea).

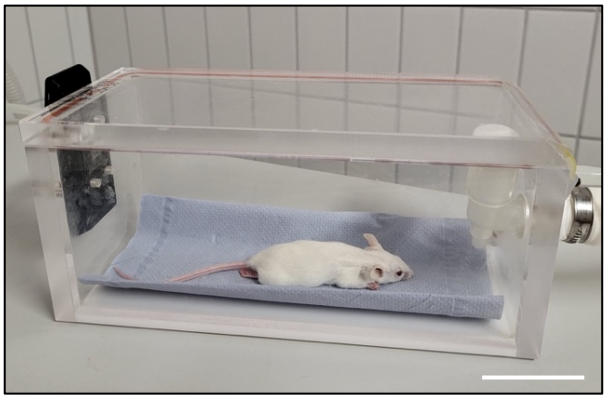

Figure 6. *Anesthetized mouse in a transparent box with narcotic gas input (right side). Scale bar: 5 cm.*

Upon application of the ultrasound gel, the scan head was linearly shifted by a three-dimensional (3D)-motor on the abdomen of the animals and two-dimensional images of the endometriotic lesions were parallely captured in intervals of 50 µm (Figure 7C). The lesions could be easily identified by their hyperechogenic suture knots at the predefined transplantation sites on the peritoneum, one in each abdominal quadrant.

To examine the ultrasound images, a three-dimensional reconstruction and analysis software was used (version VevoLAB 5.6.1; VisualSonics). In 200 µm sized steps, the borders of the lesions and their cyst-like dilated endometrial glands were identified and outlined in parallel sections. The total volume of the developing endometriotic lesions and the volume of their

stromal tissue and cysts (in mm^3) were assessed by manual image segmentation [Laschke et al., 2010]. The growth rate of the lesions and stromal tissue (in % of the initial lesion and stromal tissue volume) and the fraction of cyst-containing lesions (in % of all lesions) were also calculated.

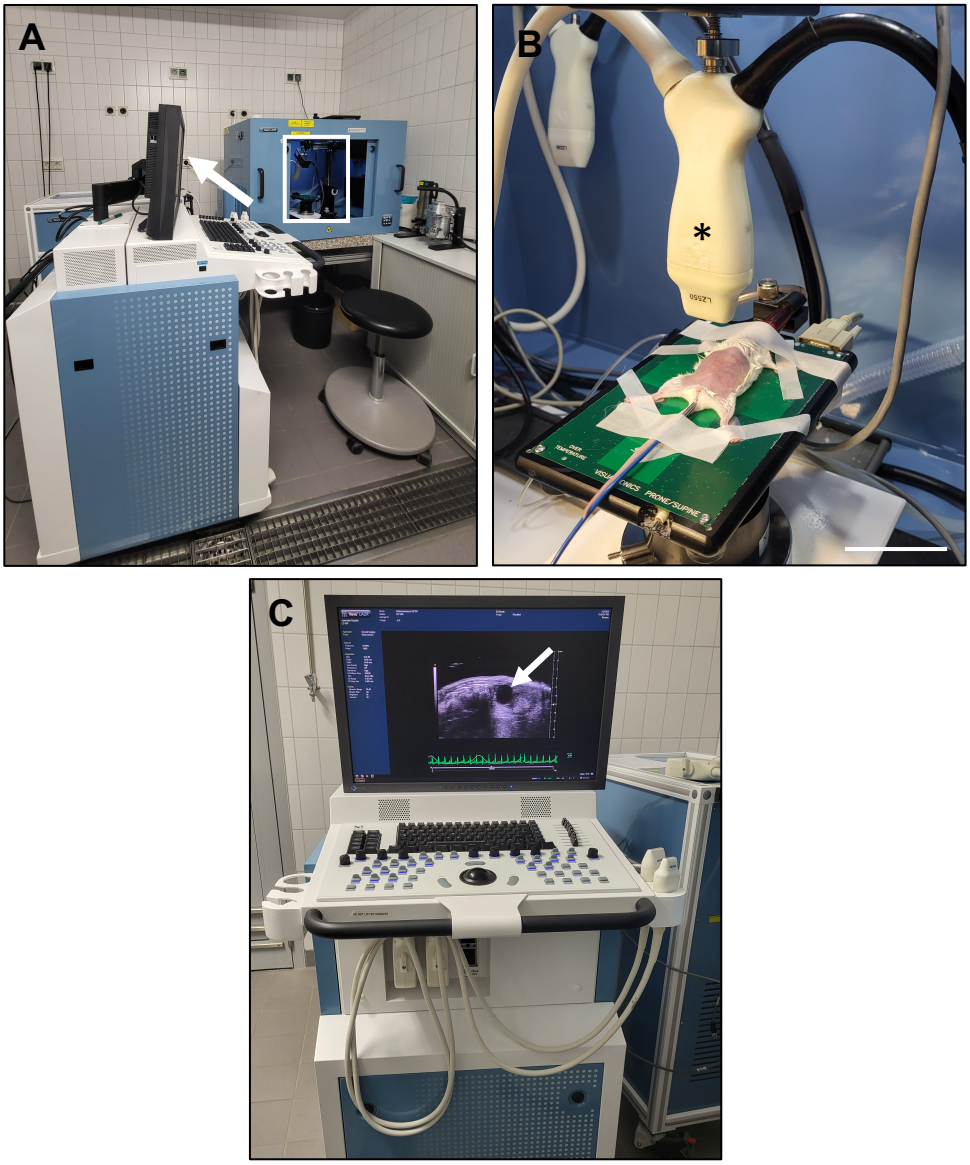

Figure 7. *High-resolution ultrasound image analysis using a Vevo LAZR system. (**A**) Vevo LAZR system from Fujifilm Visualsonics (left) and Vevo imaging station (right) with open doors. The white frame shows the perspective of view of panel B. The white arrow shows the perspective of view on the screen in panel C. On the cabinet on the right, the isoflurane vaporizer with oxygen input can be seen. (**B**) Vevo imaging station with a heated mouse platform and an anesthetized mouse fixed with tape. All paws are placed on monitor pads and a rectal thermometer probe (blue cable) is taped parallelly to the tail. The snout of the mouse is fixated into the gas mask for continuous isoflurane inhalation. The 40 MHz ultrasound transducer (∗) is placed above the mouse. Scale bar: (**B**) = 6 cm. (**C**) Vevo LAZR computer screen during the ultrasound investigation. The image of an endometriotic lesion with cyst formation is displayed on the screen (white arrow).*

5.6. Bioluminescence imaging

The luciferase activity within endometriotic lesions was visualized using bioluminescence imaging with an IVIS Spectrum In Vivo Imaging System (Perkin Elmer, Waltham, MA, USA). For this purpose, the animals were administered a subcutaneous injection of 50 mg/kg synthetic D-luciferin (CycLuc1; Tocris, Bio-Techne, Wiesbaden, Germany) in 100 µL PBS upon being anesthetized with 2% isoflurane in oxygen. Following a 5-minute incubation period to confirm the substrate's systemic distribution, the animals were positioned within the IVIS Spectrum In Vivo Imaging System (Figure 8) and imaged using the Living Image software (version 4.7.3, Perkin Elmer). The bioluminescence signal of individual lesions was measured by drawing a region of interest (ROI) over the location of the lesion. Within the chosen ROIs, the total flux was measured in photons/second (p/s). After ending the isoflurane exposure following these procedures, the animals showed a normal activity again within a few minutes.

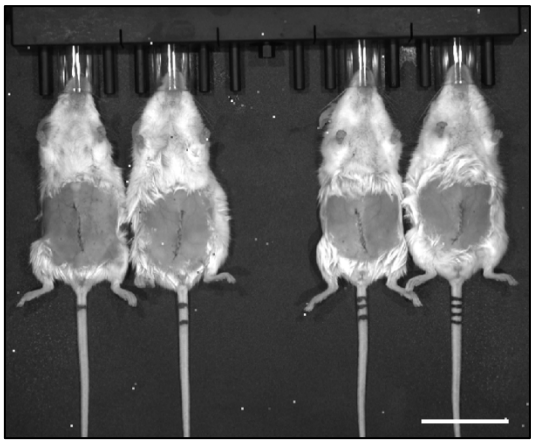

Figure 8. *Imaged FVB/N mice placed inside the IVIS Spectrum In Vivo Imaging System with gas masks for inhalational anesthesia. The laparotomy scars from the induction of endometriotic lesions are visible on the abdomens of the mice. Scale bar: 3 cm.*

5.7. Excision of endometriotic lesions

Following the in vivo experiments, the anesthetized mice were carefully laparotomized under a stereomicroscope. After identification of the endometriotic lesions on the peritoneum (Figure 9), they were harvested with microscissors. The extracted samples were fixated in paraformaldehyde for additional histological and immunohistochemical analyses. All animals were euthanized by incision of the inferior vena cava.

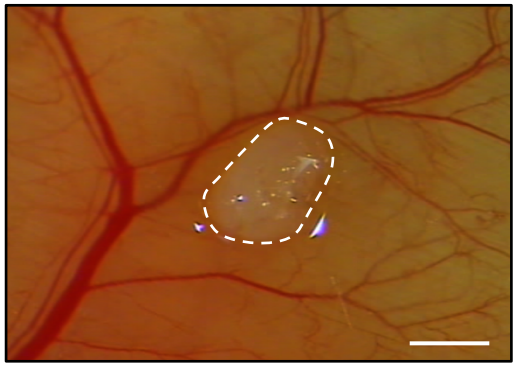

Figure 9. *A newly developed endometriotic lesion (borders marked by broken line) on the abdominal peritoneum 28 days after transplantation of uterine tissue. Scale bar: 1 mm.*

5.8. Histology and immunohistochemistry

The endometriotic lesions with the surrounding tissue were embedded in paraffin after paraformaldehyde fixation. Three-µm-thick sections were stained with hematoxylin and eosin (HE) in accordance with standard procedures. All sections were analyzed under a light microscope (BX53; Olympus, Hamburg, Germany) to assess the morphology of the endometriotic lesions. These were defined by the presence of glandular as well as stromal cells. Regressed lesions, which did not exhibit these characteristics, were defined as granuloma and excluded from further analyses (Figure 10).

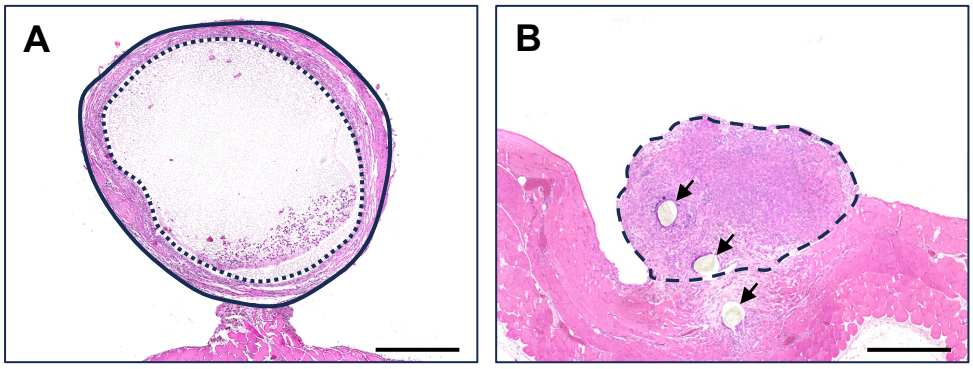

Figure 10. *HE-stained section of an endometriotic lesion (**A**) and a suture granuloma (**B**) at the implantation sites of uterine tissue samples on the abdominal peritoneum. (**A**) Endometriotic lesion with stromal and glandular components (border marked by line, cyst-like dilated endometrial gland marked by broken line). (**B**) Suture granuloma (border marked by broken line). No glandular epithelial cells are present. The rests of surgical suture material are marked (arrows). Scale bars: 350 µm.*

For the detection and quantification of proliferating cells, microvessels as well as infiltrating lymphocytes, neutrophilic granulocytes and macrophages within the lesions, several immunohistochemical stainings were performed, as described in the following sections.

5.8.1. Ki67, CD3, myeloperoxidase (MPO) and CD68 staining

All sections of endometriotic lesions were stained for the detection of the proliferation marker Ki67. Ki67 is expressed in cells during all phases of the cell-division cycle, but not in the resting phase [Scholzen & Gerdes, 2000]. Therefore, the marker is suitable to determine all dividing cells in any given cell population. The staining of the sections was performed with a rabbit polyclonal antibody against Ki67 (1:400; Cell Signaling, Leiden, The Netherlands).

CD3 is expressed in all stages of T-cell development, first in the cytoplasm and later on the cell membrane. Due to its high specificity, it is most suitable for T-cell screening of tissue sections [Alarcon et al., 1988]. For this staining, a rabbit polyclonal antibody against CD3 (1:100; Abcam, Cambridge, UK) was used.

MPO is a marker for neutrophilic granulocytes. It is an enzyme expressed by neutrophils with the purpose of destroying pathogens [Nauseef et al., 1988]. A rabbit polyclonal antibody was used for MPO detection (1:100; Abcam).

CD68 is a marker for cells of the monocyte lineage, but particularly for macrophages. It is found in the cytoplasmatic granules of these cells [Kunisch et al., 2004]. For CD68 detection, a rabbit polyclonal antibody (1:300; Abcam) was used.

As secondary antibodies for all mentioned staining procedures, a goat anti-rabbit biotinylated antibody (ready-to-use, Abcam) followed by avidin-peroxidase (ready-to-use, Abcam), was added. 3-Amino-9-ethylcarbazole (AEC Substrate System; Bio SB Inc., Santa Barbara, CA, USA) was used as chromogen followed by a counterstaining with hemalaun (Mayer's hemalaun solution; Merck KGaA, Darmstadt, Germany).

5.8.2. CD31 staining

For the detection of microvessels inside the endometriotic lesions, a monoclonal rat anti-mouse antibody against the endothelial cell marker CD31 (1:100; Dianova GmbH, Hamburg, Germany) was used. A goat anti-rat IgG Alexa555 antibody (1:100; Invitrogen, Darmstadt, Germany) was added as secondary antibody. The staining of cell nuclei was performed using Hoechst 33342 (2 µg/mL; Sigma-Aldrich).

5.8.3. Staining analysis

Using a BX53 microscope (Olympus) (Figure 11), images of the histological sections were captured in four different ROIs within the endometriotic lesions. For cell counting, the image processing program ImageJ (National Institutes of Health, LOCI, University of Wisconsin, USA) was used. Firstly, the fraction of proliferating cells (% of all visible cells) was assessed by counting the number of Ki67-positive stromal and glandular cells within the endometriotic lesions.

The numbers of CD3-positive lymphocytes, MPO-positive neutrophilic granulocytes and CD68-positive macrophages (mm^{-2}) were calculated by counting the positive cells per ROI inside of each endometriotic lesion. After manual selection of the analyzed area, ImageJ automatically calculated the number of positive cells per mm^2.

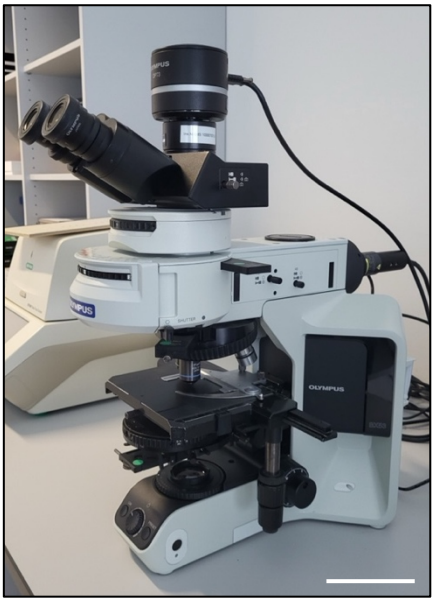

Figure 11. *The light and fluorescence microscope BX53 from Olympus with a camera attached on top for photo capturing that was used for all histological examinations of slides. Scale bar: 12 cm.*

The microvessel density (mm^{-2}) was examined by means of a BZ-8000 microscope (Keyence, Osaka, Japan). The total number of CD31-positive microvessels was counted in each analyzed area of stromal tissue and divided by that area's surface.

5.9. Peritoneal lavage

The analysis of the peritoneal fluid before and following the induction of endometriotic lesions was performed by means of a peritoneal lavage. FVB/N mice were therefore put under anesthesia by intraperitoneally injecting 100 mg/kg ketamine (Ursotamin®; Serumwerke Bernburg) and 12 mg/kg xylazine (Rompun®; Bayer). Thereafter, the peritoneal cavity was slowly injected with 2 mL of ice-cold PBS. A homogenous distribution of PBS was achieved by gentle massage of the abdomen. Two minutes later, the PBS with containing cells and soluble factors was removed using a 20G cannula (B. Braun, Melsungen, Germany), then stored on ice until further analyses.

5.10. Flow cytometry

The peritoneal fluid was centrifuged at 400×g for 5 minutes in order to separate the cellular precipitate from the supernatant. Next, the fluorescein isothiocyanate (FITC)-conjugated monoclonal rat anti-mouse granulocyte surface marker Gr-1 (ImmunoTools, Friesoythe, Germany) and the FITC-conjugated monoclonal hamster anti-mouse lymphocyte surface marker CD3ε (Immuno-Tools) were incubated with the cell suspension for 30 minutes to perform flow cytometry. Subsequently, the cells were treated by using phycoerythrin (PE)-conjugated monoclonal rat anti-mouse intracellular macrophage marker CD68 (BD Pharmingen, BD Biosciences, Heidelberg, Germany) after being fixated and permeabilized by means of BD Cytofix/Cytoperm™ Fixation and Permeabilization Solution (BD Biosciences). A FACSLyric™ system (BD Biosciences) was operated for the flow cytometric analysis and the FACSuite™ software program (version 1.3) was used to evaluate the data. Data were given as a fraction (%) of all counted cells in the peritoneal fluid.

5.11. Cytokine array

After the peritoneal fluid was centrifuged, the supernatant was collected and a proteome profiler mouse cytokine array kit (R&D Systems, Bio-Techne, Wiesbaden, Germany) was used to perform a membrane-based sandwich immunoassay. In accordance with the manufacturer's instructions, the samples were combined with a cocktail of 40 mouse biotinylated detection antibodies against cytokines, chemokines and acute phase proteins. Chemiluminescent detecting reagents allowed the visualization of the proteins. The produced

signal was proportionate to the amount of bound analyte. Data were given as mean pixel density for each measured analyte, respectively as ratio (%) of d14/d0.

5.12. Experimental protocol

For completing the first experimental part of this study, 16 uterine tissue samples from six transgenic FVB-Tg(CAG- luc-GFP)L2G85Chco/J mice and 16 uterine tissue samples from six FVB/N wild-type mice were simultaneously transplanted (ST) on day 0 (d0) into the abdomen of eight wild-type mice (Figure 12A). Two luciferase-positive and two luciferase-negative samples per mouse were surgically attached at random sites (either right cranial, right caudal, left cranial or left caudal) of the peritoneum on each side of the abdominal wall.

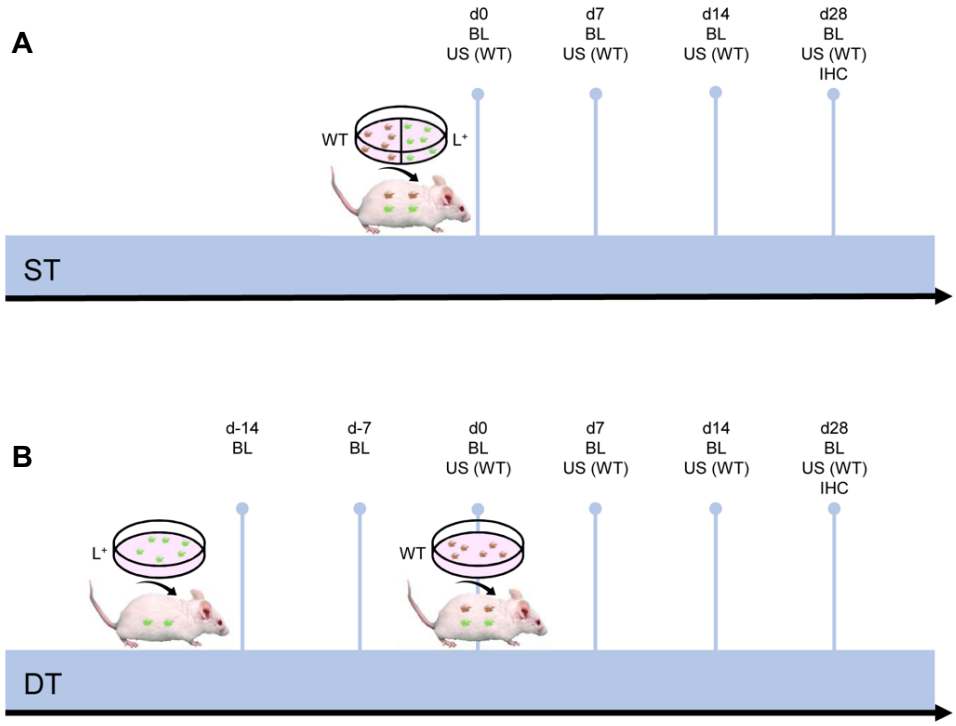

Figure 12. *The design of the study schematically illustrated. (**A**) Simultaneous transplantation (ST) of uterine tissue samples from FVB-Tg(CAG-luc-GFP)L2G85Chco/J (L^+) and FVB/N wild-type (WT) mice in the abdomen of FVB/N WT mice. (**B**) Time-delayed transplantation (DT) of uterine tissue samples from FVB-Tg(CAG-luc-GFP)L2G85Chco/J on d-14 and FVB/N WT mice on d0 in the abdomen of FVB/N WT mice. Bioluminescence (BL) was used for analysis of all lesions. Additionally, the imaging of only WT lesions as performed by using high-resolution ultrasound (US). After completing all in vivo experiments, the excision and further processing of the lesions for histology and immunohistochemistry (IHC) followed. [Mihai et al., 2023]*

For the second experimental part, a time-delayed transplantation (DT) of the transgenic and non-transgenic uterine tissue samples was performed (Figure 12B). A total of 16 uterine tissue samples from two transgenic FVB-Tg(CAG- luc-GFP)L2G85Chco/J mice were therefore transplanted to the right side of the peritoneal wall of eight recipient wild-type mice (d-14). Two weeks later (d0), a second laparotomy of the mice was performed and 16 uterine tissue samples from two FVB/N wild-type mice were transplanted to the left peritoneal wall.

The analysis of only wild-type implanted uterine tissue samples from both groups (ST and DT) was performed by repeatedly high-resolution ultrasound imaging over a 28-day observation period. All lesions developed from both luciferase-negative and luciferase-positive samples were analyzed by means of bioluminescence imaging. Subsequently, the lesions were excised and processed for histological analyses.

For the third and last experimental part, 8 uterine tissue samples originating from two transgenic FVB-Tg(CAG- luc-GFP)L2G85Chco/J mice were transplanted to the right peritoneal wall of four recipient FVB/N wild-type mice on d0. Thus, like in the DT group on d-14, each mouse was implanted with two luciferase-positive samples on the right. Before surgery, a peritoneal lavage was performed (see 5.9). Two weeks after lesion induction (d14), another peritoneal lavage was performed and the cell suspension was stored again for comparative analyses of d0 and d14.

5.13. Statistics

Every experiment was designed using blinded analysis and randomization to create equal-sized groups. All data were first examined for equal variance and normal distribution. When dealing with parametric data, an unpaired Student's t-test was utilized to evaluate group differences. When dealing with non-parametric data, a Mann-Whitney rank sum test was used to evaluate the differences among the groups. Analysis of variance (ANOVA) for repeated measurements on parametric data was performed to evaluate temporal effects within each experimental group, followed by a Tukey's post-hoc test. A Friedman's test and Dunn's post-hoc test were used to analyze non-parametric data (GraphPad Prism 9.5.1; GraphPad Software, San Diego, CA, USA). The data of this study were formulated as mean ± standard error of the mean (SEM). Statistical significance was defined for $p < 0.05$.

6. RESULTS

6.1. Development of endometriotic lesions

HE stainings verified that at least one uterine tissue sample of both transgenic and wild-type origin had ultimately developed into an endometriotic lesion in every animal of both groups (ST and DT). Endometriotic lesions were defined for when both endometrial stroma and glands were present (Figure 13A-B). Further analyses did not include completely regressed grafts which did not fulfill these conditions.

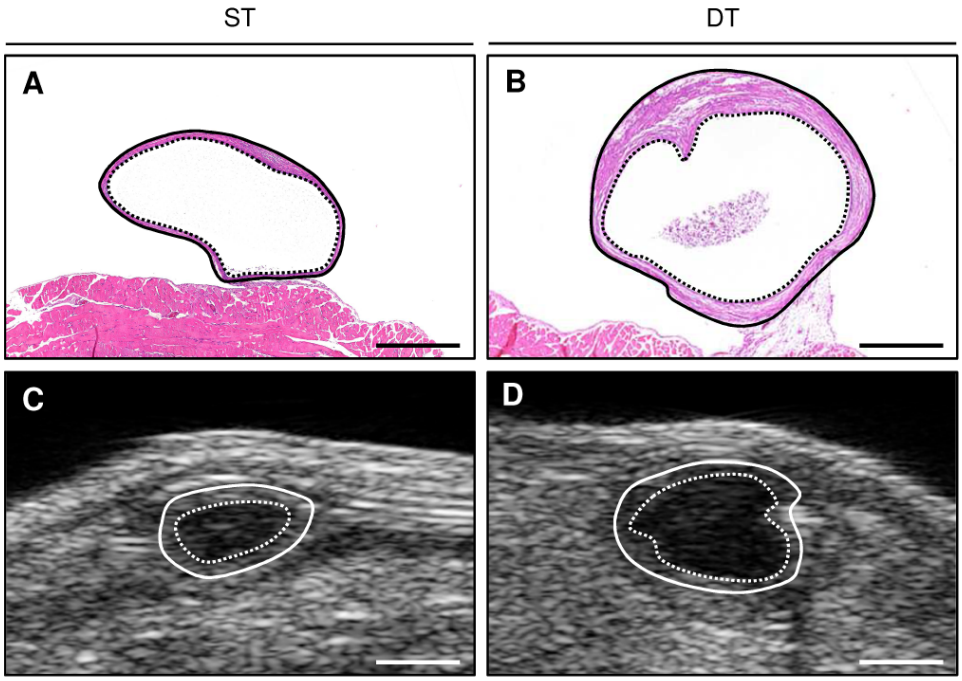

Figure 13. *Endometriotic lesions analyzed by means of histomorphology and high-resolution ultrasound imaging. (**A**,**B**) HE-stained sections of WT endometriotic lesions (lines marking borders, dotted lines marking cyst-like dilated endometrial glands) 28 days after simultaneous (ST;(**A**)) and time-delayed (DT;(**B**)) transplantation of uterine tissue samples from FVB/N WT mice into the abdomen of FVB/N WT mice. Scale bars: (**A**,**B**) = 500 µm. (**C**,**D**) WT endometriotic lesions imaged by high-resolution ultrasound (borders marked by lines, cyst-like dilated endometrial glands marked by dotted lines) 28 days after simultaneous (ST; (**C**)) and delayed (DT; (**D**)) transplantation of uterine tissue samples from FVB/N WT mice into the abdomen of FVB/N WT mice. Scale bars: (**C**,**D**) = 1 mm. [Adapted from Mihai et al., 2023]*

The developing endometriotic lesions were analyzed by use of high-resolution ultrasound imaging (Figure 13C-D, Figure 14A-F). The results of these measurements showed a comparable initial volume (d0) of ~ 1.3 mm^3 for wild-type lesions in the ST and DT group, corresponding to standard baseline conditions (Figure 14A).

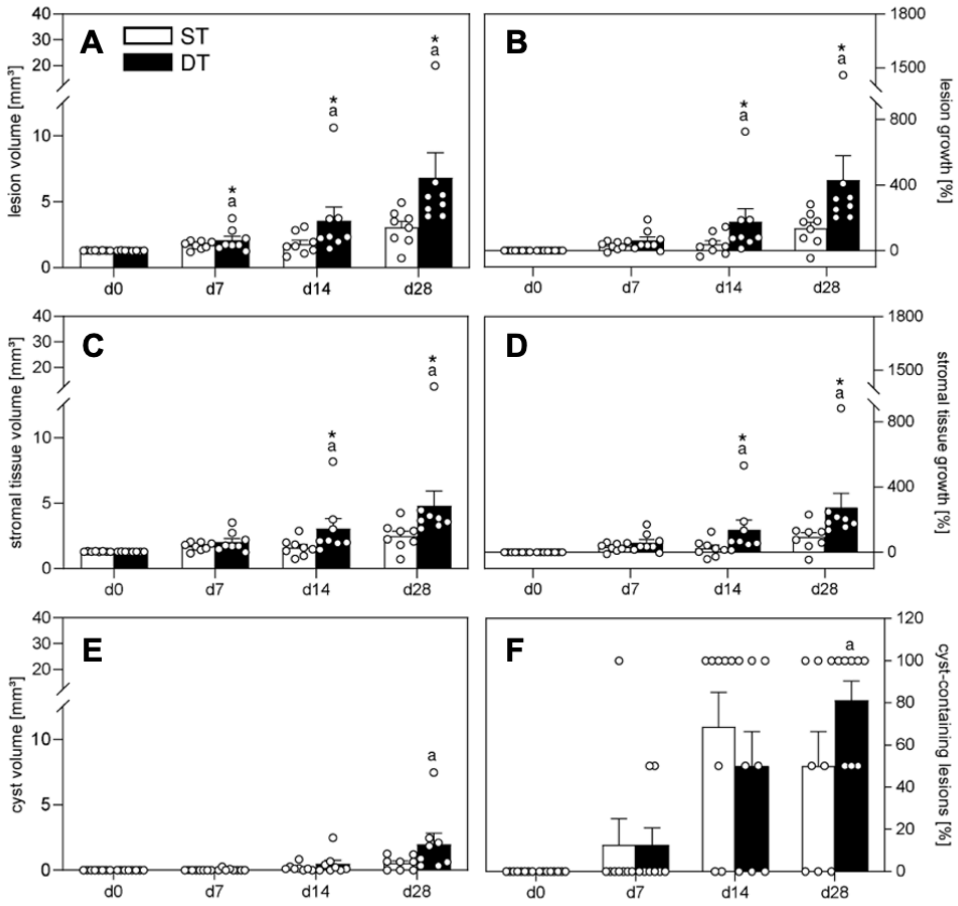

Figure 14. *Results of high-resolution ultrasound analyses in the ST and DT groups. (**A**-**F**) Lesion volume ((**A**), mm³), lesion growth (**B**, %), stromal tissue volume (**C**, mm³), stromal tissue growth (**D**, %), cyst volume (**E**, mm³) and fraction of cyst-containing lesions (**F**, %) of endometriotic lesions induced by transplantation of uterine tissue samples from FVB/N WT mice into the abdomen of FVB/N WT mice of the ST group (white bars; n = 8) and the DT group (black bars; n = 8) on days 0-28. Mean ± SEM; [a]P < 0.05 vs. d0; *P < 0.05 vs. ST. [Adapted from Mihai et al., 2023]*

However, only lesions in the DT group exhibited progressive growth and a significantly higher lesion volume, stromal tissue volume and cyst volume throughout the course of the 28-day observation period when compared to d0 (Figure 14A,C,E). Accordingly, their overall volume and stromal tissue volume grew at a faster rate when compared to the lesions in the ST group (Figure 14B,D). On the other hand, the lesions in the ST group did not remarkably grow and showed a significantly lower overall volume and stromal tissue volume between d7-d28 compared to the lesions of the DT group (Figure 14A,C). Even if the number of cyst-containing lesions increased in the DT group over time, the cyst volume did not differ in the two described groups (Figure 14E-F).

6.2. Cellular exchange between individual endometriotic lesions

The cellular exchange between endometriotic lesions was examined using bioluminescence imaging. To control whether the experimental setting was appropriate, bioluminescence imaging of FVB-Tg(CAG-luc-GFP)L2G85Chco/J and FVB/N wild-type mice as well as of their uterine horns and uterine tissue samples was first performed with and without the administration of synthetic D-luciferin. This investigation showed that the transgenic mice exhibited high levels of luciferase expression (Figure 15A-B). As expected, neither transgenic mice without being administered luciferin, nor FVB/N wild-type mice with administered luciferin showed any bioluminescence signals (Figure 15A). Similar results were observed when analyzing the ex vivo uterine horns and uterine tissue samples (Figure 15B).

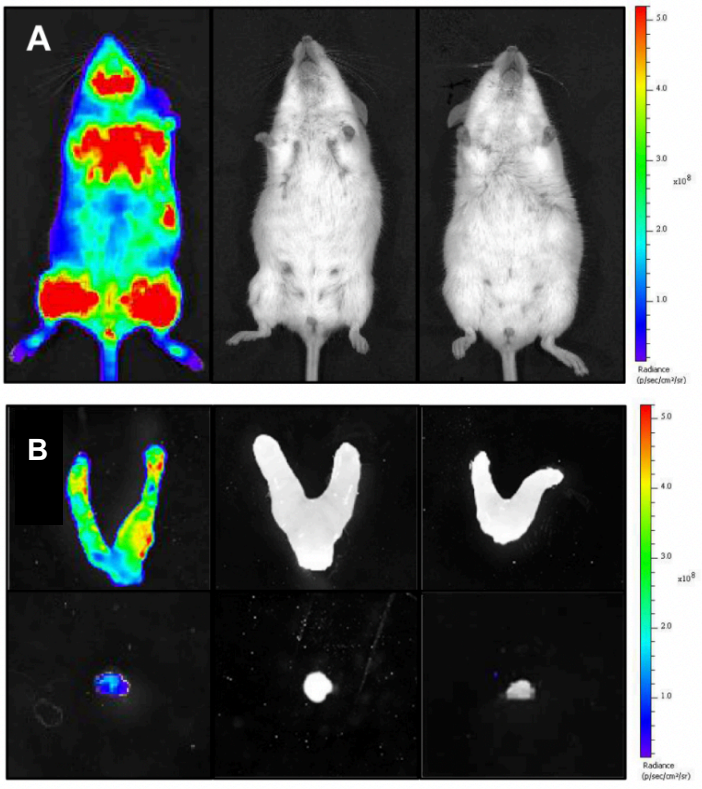

Figure 15. *Bioluminescence imaging of mice and their uterine tissue. (**A**) Left to right: FVB-Tg(CAG-luc-GFP)L2G85Chco/J mouse after injecting of synthetic D-luciferin; FVB-Tg(CAG-luc-GFP)L2G85Chco/J mouse without injecting synthetic D-luciferin; FVB/N WT mouse after injecting synthetic D-luciferin. (**B**) Left to right: Uteri (upper panel) and uterine tissue samples (lower panel) from mice in A. [Adapted from Mihai et al., 2023]*

Following the induction of endometriotic lesions, the animals in the ST and DT groups were imaged by bioluminescence once a week starting on the day of the first uterine tissue transplantation (ST: d0; DT: d-14) (Figure 16A-B). In the ST group, endometriotic lesions originating from uterine tissue samples of transgenic mice showed an increased total flux during all 28 days compared to day 0 (Figure 16C). In the DT group, the lesions of transgenic origin also showed an increased total flux during the first four weeks (d-14 to d14). After another two-week period of observation (d14 to d28), the bioluminescence signal declined to baseline values (Figure 16D). On the other hand, endometriotic lesions originating from uterine tissue samples of wild-type mice did not exhibit any signal at the anticipated locations (shown by white circles) in either group during the entire observation period (Figure 16A-D). These results suggest that no significant cellular exchange occurred between luciferase-positive and luciferase-negative lesions.

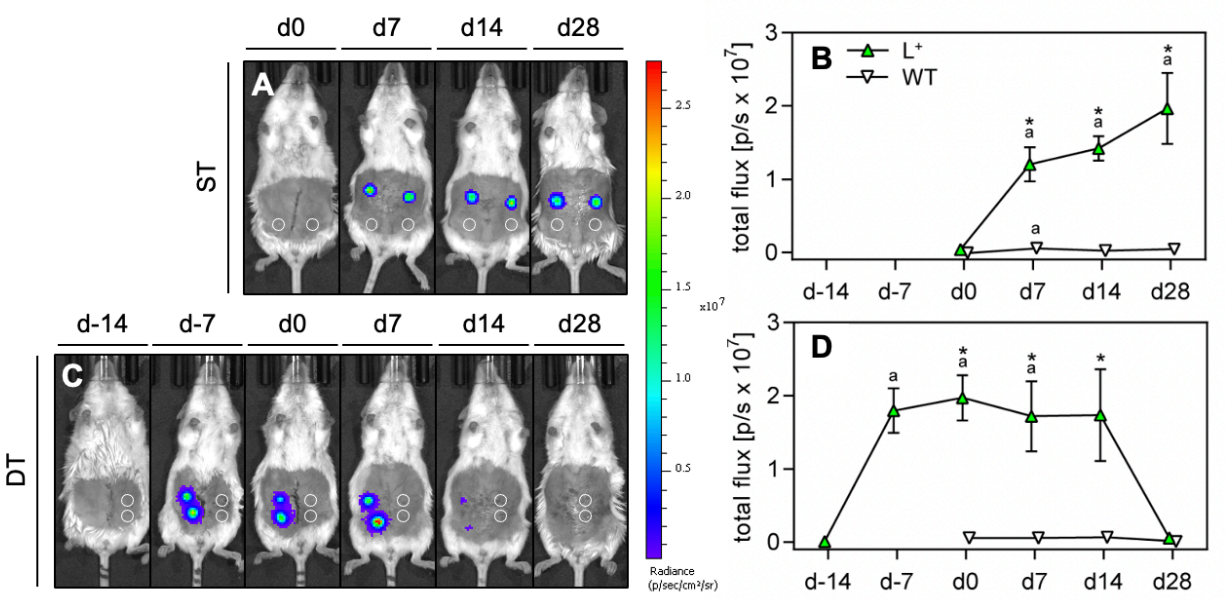

Figure 16. *Bioluminescence imaging of endometriotic lesions. (**A**) Whole body bioluminescence images of FVB/N WT mice 28 days after simultaneous transplantation (ST) of uterine tissue samples from FVB-Tg(CAG-luc-GFP)L2G85Chco/J mice and FVB/N WT mice (white circles marking their location) into the abdomen of FVB/N WT mice. (**B**) Total flux (p/s × 10^7) of bioluminescence in uterine tissue samples from FVB-Tg(CAG-luc-GFP)L2G85Chco/J mice (L+, green triangles; n = 8) and FVB/N WT mice (WT, white triangles; n = 8) after simultaneous transplantation into the abdomen of FVB/N WT mice. [a]p < 0.05 vs. d0; * p < 0.05 vs. WT. (**C**) Whole body bioluminescence images of FVB/N WT mice 28 days after time-delayed transplantation (DT) of uterine tissue samples from FVB-Tg(CAG-luc-GFP)L2G85Chco/J mice (d-14) and FVB/N WT mice (d0) (white circles marking their location) into the abdomen of FVB/N WT mice. (**D**) Total flux (p/s × 10^7) of bioluminescence in uterine tissue samples from FVB-Tg(CAG-luc-GFP)L2G85Chco/J mice (L+, green triangles; n = 8) and FVB/N WT mice (WT, white triangles; n = 8) after time-delayed transplantation into the abdomen of FVB/N WT mice. [a]p < 0.05 vs. d-14; * p < 0.05 vs. WT. [Adapted from Mihai et al., 2023]*

6.3. Vascularization, proliferation and immune cell infiltration of endometriotic lesions

Following all in vivo experiments, immunohistochemical staining was performed to evaluate the vascularization, proliferation and immune cell infiltration of the wild-type lesions in the ST and DT groups. It was found that the density of CD31-positive microvessels was comparable between lesions of both groups (Figure 17A-C).

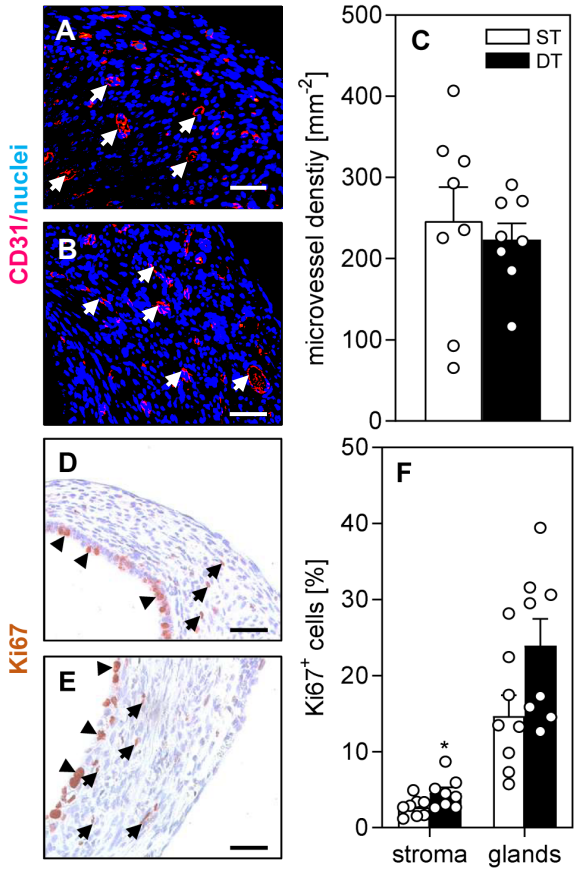

Figure 17. *The vascularization and proliferation of endometriotic lesions analyzed by immunohistochemstryl. (**A**,**B**) Immunofluorescent detection of microvessels (arrows) in WT endometriotic lesions on day 28 following simultaneous (ST; (**A**)) and time-delayed (DT; (**B**)) transplantation of uterine tissue samples from FVB-Tg(CAG-luc-GFP)L2G85Chco/J mice and FVB/N WT mice into the abdomen of FVB/N WT mice. The immunohistochemical sections were stained with an antibody against CD31 for the detection of microvessels (red). Cell nuclei appear blue. Scale bars: 50 µm. (**C**) Microvessel density (mm^{-2}) of endometriotic lesions induced by transplantation of uterine tissue samples from FVB/N WT mice into the abdomen of FVB/N WT mice in the ST group (white bars; n = 8) and DT group (black bars; n = 8). Mean ± SEM. (**D**,**E**) Immunohistochemical detection of Ki67-positive stromal cells (arrows) and glandular epithelial cells (arrowheads) in WT lesions on day 28 following simultaneous (ST; (**D**)) and time-delayed (DT; (**E**)) transplantation of uterine tissue samples (idem (A,B)). The immunohistochemical sections were stained using an antibody against Ki67 for the detection of proliferating cells (brown). Scale bars: 50 µm. (**F**) Ki67-positive cells (% of all cells) in the stroma and the glands of endometriotic lesions induced by transplantation of uterine tissue samples (idem (C)) in the ST group (white bars; n = 8) and DT group (black bars; n = 8). Mean ± SEM. * $p < 0.05$ vs. ST. [Mihai et al., 2023]*

Of interest, a significantly higher fraction of proliferating Ki67-positive stromal cells was found within the lesions of the DT group compared to the ST group (Figure 17D-F). In contrast, no significant difference could be identified concerning the glandular cells (Figure 17D-F).

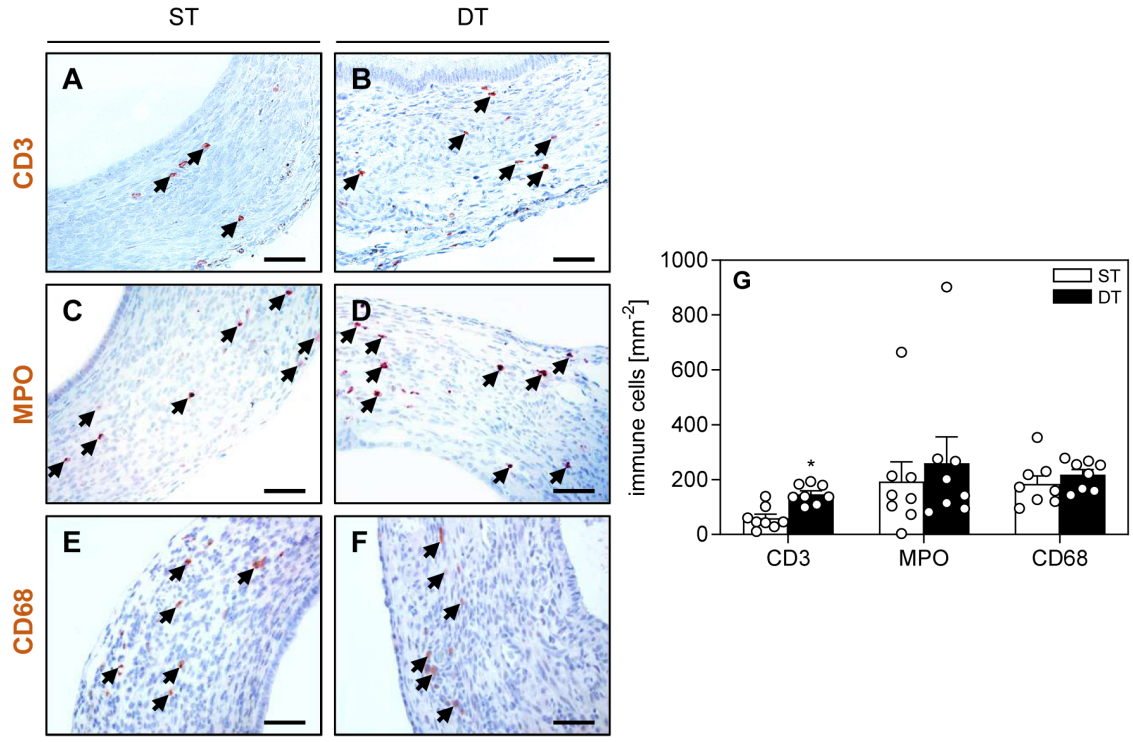

Figure 18. *The immune cell infiltration of endometriotic lesions by immunohistochemistry. (**A**–**F**) Immunohistochemical detection of CD3-positive lymphocytes ((**A**,**B**); arrows), MPO-positive neutrophilic granulocytes ((**C**,**D**); arrows) and CD68-positive macrophages ((**E**,**F**); arrows) in the stromal tissue of WT endometriotic lesions on day 28 following simultaneous (ST; (**A**,**C**,**E**)) and time-delayed (DT; (**B**,**D**,**F**)) transplantation of uterine tissue samples from FVB-Tg(CAG-luc-GFP)L2G85Chco/J mice and FVB/N WT mice into the abdomen of FVB/N WT mice. Scale bars: 50 µm. (**G**) CD3-positive lymphocytes (mm^{-2}), MPO-positive neutrophilic granulocytes (mm^{-2}) and CD68-positive macrophages (mm^{-2}) in WT endometriotic lesions induced by transplantation of uterine tissue samples into the abdomen of FVB/N WT mice in the ST group (white bars; n = 8) and DT group (black bars; n = 8). Mean ± SEM; * $p < 0.05$ vs. ST. [Mihai et al., 2023]*

Next, the amount of CD3-positive lymphocytes, myeloperoxidase (MPO)-positive neutrophilic granulocytes and CD68-positive macrophages was measured (Figure 18A-G). This analysis revealed that there were significantly more lymphocytes within the wild-type lesions in the DT group in comparison with those in the ST group (Figure 18A-B, G). However, the numbers of neutrophilic granulocytes and macrophages did not differ in the two groups (Figure 18C-G).

6.4. Immune cells and inflammatory factors in the peritoneal fluid before and after induction of endometriotic lesions

In a last series of experiments, a peritoneal lavage was performed in four healthy FVB/N wild-type mice (baseline condition). To examine the impact of newly developing endometriotic lesions on the physiological environment of the abdomen, two uterine tissue samples from two FVB-Tg(CAG-luc-GFP)L2G85Chco/J donor mice were then sutured to the right abdominal wall of each mouse and a second peritoneal lavage was carried out 14 days later.

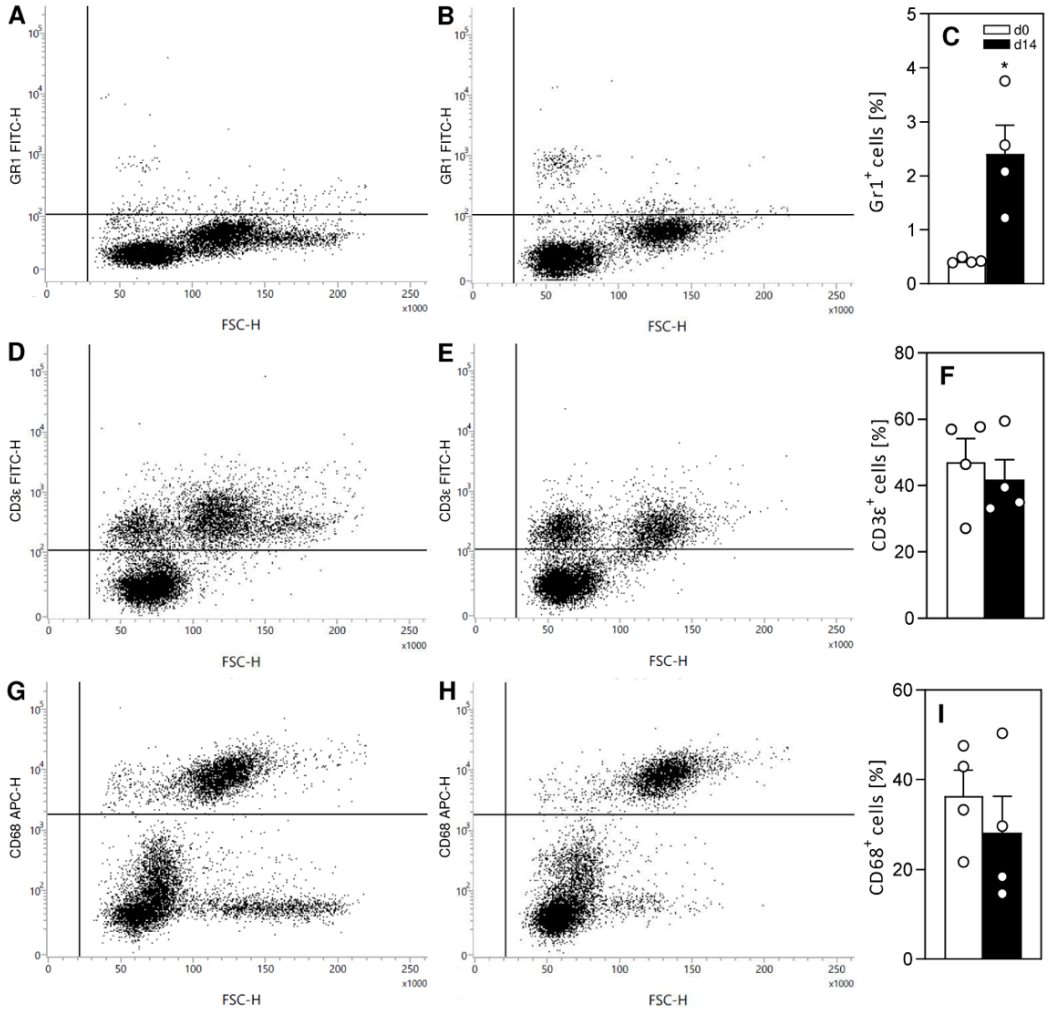

Figure 19. *Flow cytometry results after processing of the peritoneal fluid. (**A**,**B**,**D**,**E**,**G**,**H**) Representative scatter plots of flow cytometric analyses of the peritoneal fluid before (d0; (**A**,**D**,**G**)) and 14 days after (d14; (**B**,**E**,**H**)) transplantation of uterine tissue samples from FVB-Tg(CAG-luc-GFP)L2G85Chco/J mice into the abdomen of FVB/N WT mice. The cell staining was performed using markers against Gr1 (granulocytes; (**A**,**B**)), CD3ε (lymphocytes; (**D**,**E**)) and CD68 (macrophages; (**G**,**H**)). (**C**,**F**,**I**) Fraction (%) of Gr1-positive granulocytes (**C**), CD3ε-positive lymphocytes (**F**) and CD68-positive macrophages (**I**) in the peritoneal fluid of FVB/N WT mice before (d0; white bars; n = 4) and 14 days after (d14; black bars; n = 4) transplantation of uterine tissue samples from FVB-Tg(CAG-luc-GFP)L2G85Chco/J mice into the abdomen of FVB/N WT mice. Mean ± SEM; * $p < 0.05$ vs. d0. [Mihai et al., 2023]*

The obtained peritoneal fluid underwent further processing for flow cytometric and protein array analyses. These revealed a significantly higher fraction of Gr1-positive neutrophilic granulocytes within the peritoneal fluid 14 days following the induction of endometriotic lesions (Figure 19A-C). In contrast, there were no marked differences between the fractions of CD68-positive macrophages and CD3ε-positive lymphocytes before and after the induction of the lesions (Figure 19D-I).

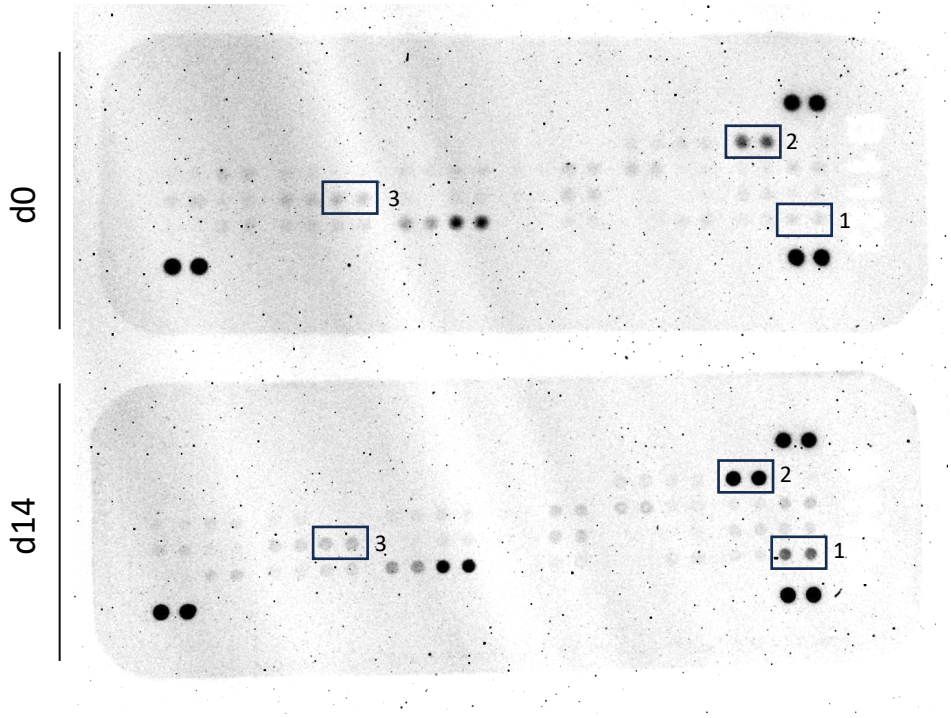

Figure 20. *Proteome profiler mouse cytokine array. The quantification was carried out via capturing the average spot pixel density. Using a coordinate system, the localization of the assessed inflammatory factors could be identified. Black boxes enclose the coordinates of detected cytokines where higher expression was measured on d14 when compared to d0 (see Table 1), showing visually darker signals on d14. Box 1: BLC* (CXCL13); box 2: TIMP-1; box 3: IL-16.

Moreover, a proteome profiler mouse cytokine array was used to measure the expression of 40 different cytokines, chemokines and acute phase proteins in the peritoneal fluid (Figure 20). Interestingly, it could be observed that, in comparison to baseline conditions, the expression of the majority of these inflammatory factors increased after 14 days following the induction of endometriotic lesions (Table 1). BLC (also referred to as CXCL13), IL-23, TIMP-1, IL-1b and IL-5 exhibited the highest elevation in expression, but only TIMP-1 and IL-5 showed statistical significance. When compared to baseline conditions, IL-2 and C5/C5a-convertase were the two cytokines with the most downregulated expression (Table 1).

Protein	Mean pixel density (Mean ± SEM)	Mean pixel density (Mean ± SEM)	Ratio d14/d0
	d0	d14	(%)
BLC (CXCL13)	3,139 ± 457	11,347 ± 5,196	361
IL-23	2,608 ± 387	5,955 ± 799	228
TIMP-1	17,609 ± 6,297	38,341 ± 8,289	217 *
IL-1b	2,742 ± 414	5,809 ± 1,851	211
IL-5	2,054 ± 607	4,313 ± 575	210 *
MCP-5	2,515 ± 943	4,970 ± 800	197
IL-16	5,427 ±1,826	10,451 ± 5,466	192
IL-12p70	2,475 ± 652	4,381 ± 922	177
I-309	2,868 ± 659	4,896 ± 991	170
IL-17	3,583 ± 988	6,103 ± 1,791	170
IP-10	3,483 ± 1,227	5,395 ± 1,361	154
IL-4	2,545 ± 683	3,873 ± 492	152
IL-3	3,107 ± 579	4,304 ± 1,164	138
IFN-gamma	9,087 ± 1,316	12,272 ± 3,164	135
ICAM-1	24,038 ± 8,847	31,685 ± 8,232	131
G-CSF	4,973 ± 784	6,291 ± 2,001	126
IL-1a	4,120 ± 514	5,041 ± 1,157	122
IL-10	3.148 ± 1,159	3,836 ± 1,130	121
IL-7	3,724 ± 857	4,445 ± 1,501	119
MIP-1a	3,084 ± 549	3,533 ± 835	114
TARC	3,200 ± 1,,242	3,481 ± 930	108
JE	4,832 ± 2,132	5,195 ± 833	107
IL-6	2,701 ± 1,058	2,894 ± 518	107
M-CSF	4,425 ± 1,579	4,660 ± 1,964	105

Eotaxin	4,012 ± 789	4,215 ± 804	105
TREM-1	2,833 ± 325	2,956 ± 789	104
RANTES	4,670 ± 1,873	4,866 ± 1,422	104
MIP-2	3,553 ± 718	3,610 ± 901	101
MIG	4,083 ± 973	4,129 ± 905	101
SDF-1	3,447 ± 348	3,480 ± 750	100
IL-27	4,651 ± 1,237	4,307 ± 1,550	92
MIP-1b	3,268 ± 722	2,887 ± 447	88
IL-13	3,276 ± 814	2,672 ± 690	81
GM-CSF	3,066 ± 766	2,416 ± 526	78
I-TAC	5,839 ± 1,395	4,521 ± 962	63
TNF-a	3,478 ± 1,067	2,629 ± 1,019	59
KC	3,109 ± 742	2,310 ± 760	54
IL-1ra	10,822 ± 6,491	5,344 ± 1,213	50
C5/C5a	6,910 ± 516	2,819 ± 607	46 *
IL-2	6,513 ± 1,015	2,259 ± 562	42 *

Table 1. *The expression of inflammatory factors in the peritoneal fluid before (d0) and 14 days (d14) after induction of endometriotic lesions, as analyzed by a proteome profiler mouse cytokine array. Data are shown as mean pixel density ± SEM (n = 4) of two technical replicates and as ratio d14/d0 in %. * p < 0.05 vs. d0. [Mihai et al., 2023]*

6.5. Summary of results

The results of the present thesis can be summarized as follows:

1. The presence of pre-existing endometriotic lesions in the peritoneal cavity promotes the growth of new lesions. In fact, it was found that the wild-type lesions of the DT group progressively grew when compared to day 0. Moreover, these lesions showed a significantly higher lesion volume than the lesions of the ST group, as assessed by repeated high-resolution ultrasound imaging. In contrast, the lesions of the ST group did not notably grow and showed a lower total volume when compared to the endometriotic lesions of the DT group. Comparable results were observed for the stromal tissue volume in both groups. Additionally, the cyst-containing lesions of the DT group increased over

time. These findings were supported by the results of additional immunohistochemical analyses. They showed a higher fraction of proliferating cells in the lesions of the DT group in comparison with those of the ST group.

2. A cellular exchange between individual endometriotic lesions could not be detected. Bioluminescence imaging showed the luminescent activity of FVB-Tg(CAG-luc-GFP)L2G85Chco/J cells in induced luciferase-positive lesions after the injection of D-luciferin. However, there was no ectopic signal outside these lesions, neither in any wild-type lesion, nor at any other site of the animals' bodies.

3. Pre-existing endometriotic lesions in the peritoneal cavity provoke a local inflammatory response. This finding was supported by the immunohistochemical analyses, revealing an increased number of CD3-positive lymphocytes that infiltrated the lesions of the DT group. The performed flow cytometric analysis revealed a higher number of Gr1-positive granulocytes in the peritoneal fluid 14 days after lesion induction when compared to baseline conditions. Additionally, a cytokine array showed a significantly elevated expression of TIMP-1 and IL-5 in the peritoneal fluid after the induction of endometriosis.

7. DISCUSSION

7.1. Discussion of materials and methods

7.1.1. Endometriosis mouse model

The present thesis analyzed the effects of pre-existing endometriotic lesions on the growth of new ones by means of an endometriosis mouse model. Endometriosis is an estrogen-dependent disease of the female reproductive system [Chantalat et al., 2020]. According to the implantation theory of Sampson [1927], endometriotic lesions develop from retrogradely shed endometrial tissue into the peritoneal cavity. However, this process is only present in humans and non-human primates. The latter have a menstrual cycle very similar to humans in its duration and endometrial remodeling. Non-human primates also have a similar reproductive anatomy to humans and develop endometriosis spontaneously [Braundmeier & Fazleabas, 2009]. Nevertheless, the primate model raises financial and ethical issues due to the large size of the animals, the costs of their housing and their behavioral similarity to humans. This leads to the preference of murine models. Laboratory mice are small in size, while also easy and cost-effective to maintain and breed. Therefore, large groups of mice can be used, resulting in a better reliability of the experiments. The physiological and genetic similarity of mice to humans has been proven before as well [Bryda, 2013; Breschi et al., 2017].

However, the limitations of the used model must also be mentioned. Mice are mammals that, unlike humans, do not develop endometriosis spontaneously. This is due to the fact that they do not menstruate, since they exhibit an anatomical difference in their reproductive system. The tubo-ovarian junction is contained in a membrane (bursa), which prevents retrograde flow from the uterine cavity to the peritoneum [Burns et al., 2022]. Therefore, iatrogenic induction of endometriotic lesions is necessary. This approach has the disadvantages of an invasive procedure, including the risk of postoperative infection and increased stress for the animals. The peritoneal environment can also be altered by opening the abdominal cavity, inducing inflammation through manipulation and sutures. Additionally, the lesion induction in this work was performed with the use of tissue samples collected from healthy donor mice and not by transplantation of endometriotic tissue of human origin into immunocompromised mice [Grümmer et al., 2001]. Results may therefore not directly correlate to human endometriosis concerning hormonal or immunological factors. Moreover, regarding the experimental protocol, the mice in the DT group underwent time-delayed surgeries, meaning two

procedures instead of a single one (like in the ST group). This implies that the mice in the DT group were exposed to more stress, possibly impacting the described results.

Another factor that could have influenced the development of endometriotic lesions from uterine tissue samples is the used synthetic suture material. The sutures were used to fixate the tissue samples to the abdominal wall and possibly triggered a foreign body reaction. In the histological sections of granuloma, where no endometriotic glands were found, the immune cell infiltration was evident. This suggests that the infiltration of the analyzed endometriotic lesions may have been promoted by the sutures. Therefore, the presence of the suture material could have further accentuated the lesion-induced inflammation in the abdominal peritoneum.

An alternative to the suture method is the injection of an endometrial cell suspension into the peritoneal cavity of mice [Burns et al., 2022]. However, this approach would have led to an arbitrary distribution of cells and development of lesions, which would have markedly complicated their sonographic identification and monitoring during the experiments of this study. Additionally, the subcutaneous placement model is another option of endometriotic lesion induction [Burns et al., 2022; Ferrero et al., 2017]. This model involves the placement of uterine tissue samples into subcutaneous pockets created between the peritoneum and the inner abdominal muscle layer. The sonographic identification of the developed lesions is facilitated by the defined location of the created pockets and no sutures are needed. However, the lesions form outside of the peritoneal cavity, making the model unfit for studying the pathophysiology of the human disease. Hence, the surgical induction of endometriotic lesions by transplantation of uterine tissue samples to the peritoneum was the preferred method in the present work.

The possibility of rejection of the transplanted tissue samples by the recipient mice was excluded by means of syngeneic transplantation. The recipient mice of the wild-type FVB/N strain were therefore implanted with uterine tissue samples from either the same wild-type strain or from the FVB-Tg(CAG-luc-GFP)L2G85Chco/J strain. Although the latter is a transgenic strain, it was bred on FVB/N background. This ensures a high level of tolerance in the recipient mice during transplantation experiments, as seen in other transplantation studies using the same mouse model [Sheikh et al., 2007].

To further eliminate confounding factors in the present work, the variability in sex hormone levels had to be controlled. Consequently, all animals in this study underwent vaginal lavage to determine their estrous cycle stage before being selected as either donor or recipient. Only mice in the estrus stage were selected for the experiments. According to Yip et al. [2013], the

estrus stage in mice exhibits molecular changes similar to the late secretory and menstrual stages in human females. Thus, the use of mice in the estrus stage aimed to replicate the humoral conditions of the human peritoneal cavity immediately before the development of endometriotic lesions via retrograde menstruation, increasing the validity of the endometriosis mouse model.

The uterine tissue samples of transgenic origin transplanted to the peritoneal wall of wild-type mice was derived from FVB-Tg(CAG-luc-GFP)L2G85Chco/J mice. This tissue, expressing firefly luciferase, was used to enable the monitoring of cell migration via bioluminescence imaging. This method allowed to test the hypothesis of whether endometriotic lesions exchange different types of cells to support their growth. Since the transgenic mouse strain has its origin in the FVB/N strain, a high immunological tolerance of recipients is possible during the performed transplantation experiments. However, at some point of the observation period (starting with the 4th week after induction), the bioluminescent activity of the luciferase-positive endometriotic lesions decreased until reaching baseline values. In line with this finding, Dorning et al. [2021] reported how, by the time of 6 weeks, lesions of the same transgenic origin (transplanted into FVB/N wild-type mice as well) either gradually decreased in size or spontaneously resolved altogether. They attributed this finding to the fact that endometriotic lesions can naturally degrade and suffer fibrosis. Still, a delayed reaction of immune intolerance could also be speculated.

7.1.2. Methods of investigation

The growth of the induced endometriotic lesions in this thesis was monitored by means of high-resolution ultrasound. This allowed for repeated non-invasive examination of the mice, keeping their stress levels to a minimum through careful handling, inhalational anesthesia and continuous monitoring of their temperature, heart and respiratory rate. This setting with the use of isoflurane gas was more appropriate than an injectional anesthesia and could guarantee the anesthesia of mice for a controlled period of time (ca. 20 min per mouse), after which they quickly recovered when isoflurane inhalation terminated. Gas anesthesia is more controllable due to the rapid drug elimination by the lung via expiration, without being metabolized. Hence, the anesthesia quickly wears off after gas administration is stopped. The shaving of the abdominal fur of the mice was performed after anesthesia induction, further minimizing stress exposure. During anesthesia, body temperature may drop and the use of ultrasound gel increases this risk. To prevent this, all animals were placed on a heated stage.

The time and skills required from the examiner to identify the lesions during ultrasound examination were reduced by the implantation of uterine tissue samples fixated by sutures in defined sites on the peritoneum wall of the recipient mice. This allowed their easy identification for the high-resolution ultrasound analyses [Rudzitis-Auth et al., 2021], because the suture produced an unnatural hyperechogenic signal during imaging. Upon collecting all imaged data at the end of the experiments, lesion growth was assessed by calculation of the total volume using a three-dimensional reconstruction and analysis software. The examiner was needed to outline the lesions and their cysts in order to obtain the calculated stroma, cyst and total volumes. The quality of this method is supported by the low intra- and interobserver variability of volume measurements [Laschke et al., 2010]. Volume measurements by use of high-resolution ultrasound corresponded visually to all analyzed histologic sections. Through this reliable method, the present work could show that pre-existing endometriotic lesions lead to a more rapid and pronounced growth of new lesions.

Another technique used for analysis was in vivo bioluminescence imaging. This allowed to monitor any existing cellular exchange between endometriotic lesions. As well as for the ultrasound investigations, the animals could be imaged repeatedly every week, providing a dynamic insight into the development of the luminescent lesions and cell migration. The developed luciferase-positive lesions in recipient mice could be imaged due to the bioluminescent activity of their cells, since the transplanted tissue originated from transgenic FVB-Tg(CAG-luc-GFP)L2G85Chco/J donors. The luminescent effect was induced by subcutaneous injection of luciferin. This was due to a reaction that takes place between the luciferin and the firefly luciferase expressed by the transgenic tissue. The mice were injected and imaged during ongoing isoflurane anesthesia, lowering stress levels accordingly. As a result, potential cell migration would be demonstrated by the identification of luminescent cells infiltrating newly developing luciferase-negative wild-type lesions.

Both imaging technologies could be used repeatedly in a non-invasive manner. This could markedly reduce the number of mice required for this study, which conformed to the 3R principle. This 3R principle sets an animal protection goal to reduce animal experiments as much as possible, following three concepts: replacement (looking for suitable alternatives instead of animal models), reduction (minimizing the number of animals used) and refinement (keeping the animal stress and suffering at a minimum) (European Directive 2010/63/EU).

7.2. Discussion of results

The pathophysiology of endometriosis has been tightly linked to repeated retrograde menstruation. The transportation of endometrial tissue into the abdomen leads to the development of endometriotic lesions and induction of an inflammatory environment [Riccio et al., 2018]. While it has not been definitively clarified whether an aberrant immune response is the cause or the result of endometriosis, the evolution of the disease is known to rely on the recruitment of a diversity of immune cells. As a result, inflammation and angiogenesis are triggered through the secretion of cytokines and growth factors. This raises the hypothesis that such a biochemically modified medium could promote the growth of new endometriotic lesions in addition to previously existing ones. In this case, the condition would progress in the manner of a vicious circle. As a confirmation for this theory, the present thesis could demonstrate that the presence of pre-existing endometriotic lesions promotes the development of new lesions in the abdomen of mice.

The growth of endometriotic lesions was quantified through separate measurements of stromal and cyst volume by means of high-resolution ultrasound. This method provided further insights into the tissue proliferation rate and secretory activity of endometriotic lesions. In fact, the wild-type endometriotic lesions in the DT group showed a significantly higher growth rate in comparison with those in the ST group. After all in vivo experiments, immunohistochemistry analyses of the lesions confirmed these findings on a cellular level, displaying a higher number of proliferating Ki67-positive cells in the stroma of the lesions in the DT group compared to the ST group.

In order to test whether cell migration was a contributing factor to the increased growth rate of endometriotic lesions in the DT group, bioluminescence imaging was performed. This method has been previously described in other mouse endometriosis studies [Becker et al., 2006; Dorning et al., 2021; Wibisono et al., 2022]. In the present mouse model, an increasing total flux was detected in luciferase-positive lesions of both the ST and DT group throughout the first 28 days after endometriosis induction. Following this period, the bioluminescence signal in the DT group progressively decreased. As mentioned above, former studies have also described an initial increase of bioluminescence signals in lesions, followed by a gradual loss of luminescent activity at later time points [Dorning et al., 2021; Wibisono et al., 2022]. This finding corresponds to the changing nature of endometriotic lesions, knowing that red lesions with increased vascularization eventually regress into white, scarred lesions [Nisolle & Donnez, 1997]. Since the luciferase-positive lesions of the DT group in the present thesis were

monitored for a longer period of six weeks (d-14 to d28), time alone could have determined the cells of the lesions to degrade and no longer emit any bioluminescent signals.

The analyses further showed that endometriotic lesions originating from wild-type uterine tissue samples exhibited no bioluminescence signals in the course of the total observation period. This demonstrates how no relevant migration of luciferase-positive cells into luciferase-negative lesions occurred. Hence, after rejection of the cell exchange hypothesis, it was assumed that other mechanisms, such as an altered inflammatory peritoneal environment, are responsible for the higher growth rate of endometriotic lesions in the DT group.

To test this concept, inflammatory factors and immune cells were assessed next in the peritoneal fluid before and after the induction of endometriotic lesions. Fourteen days after the induction of endometriotic lesions in mice, there was an increase in the expression of most pro-inflammatory cytokines analyzed in the peritoneal fluid using a proteome profiler mouse cytokine array. Previous studies have shown that several of these factors contribute to the pathophysiology of endometriosis. For example, a significant upregulation of IL-5 was found, which is indicative of early-stage endometriosis. IL-5 generally aids in the survival, proliferation and differentiation of several cell types [Jorgensen et al., 2017; Monsanto et al., 2016]. It is particularly known for supporting the survival and priming of matured eosinophil granulocytes [Hassani & Koenderman, 2018]. The IL-5 levels positively correlated with the flow cytometry results, revealing a significantly higher fraction of granulocytes in the peritoneal fluid after 14 days following the lesion induction.

Studies in patients with endometriosis have shown that granulocyte numbers are higher in the peritoneal fluid compared to healthy women [Milewski et al., 2011; Symons et al., 2018]. Granulocytes play a role in the pathogenesis of endometriosis by promoting fibrous adhesions after degranulation. Interestingly, Hornung et al. [2000] described how eotaxin, a chemoattractant for eosinophils, is expressed by the eutopic endometrium of women with endometriosis, leading to endometrial dysfunction, impaired implantation and infertility. Thus, elevated levels of eosinophilic granulocytes or eotaxin in the peritoneal fluid might be a prognostic factor for the aggressiveness of the disease [Vallvé-Juanico et al., 2019]. In addition, it is known that IL-17, IP-10 (CXCL10) and IL-23 promote inflammation in endometriosis by facilitating granulocyte migration [Andreoli et al., 2011; Izumi et al., 2018]. In line with this, the present study found that these cytokines were also increased in the peritoneal fluid of mice with endometriotic lesions.

Immunohistochemical staining of the wild-type lesions was performed 28 days after endometriosis induction to assess immune cell infiltration. This analysis revealed a similar

fraction of macrophages and granulocytes in the lesions of both the ST and DT group. However, significantly more CD3-positive lymphocytes were detected in the lesions of the DT group compared to the ST group. This finding aligns with the increased expression of IL-23 and IL-17 in the peritoneal fluid, since these cytokines are known to be secreted by activated T-lymphocytes [Shi et al., 2022]. IL-17, secreted by Th17 helper cells, has also been linked to endometriosis in previous works. Th17 cells were increased in the peritoneal fluid as well as in the peripheral blood of women with endometriosis. The levels of the analyzed cells correlated with the disease severity [Gogacz et al., 2016]. Correspondingly, IL-17 plasma levels have been shown to decrease after surgical removal of lesions [Ahn et al., 2015]. While IL-17 plays an important role in enhancing inflammation and angiogenesis, it has not been sufficiently studied to fully understand its relevance in terms of an immune system dysfunction in endometriosis. Furthermore, in line with the presented results of the cytokine array, IL-23 is also involved in the pathophysiology of endometriosis and the Th17/IL-17 axis. IL-23 has been described as an essential contributor to the development and differentiation of Th17 cells [Sisnett et al., 2023].

The highest cytokine level detected in this thesis was for BLC. This finding is in line with the results of Franasiak et al. [2015], who demonstrated that BLC (referred to as CXCL13 in their study) expression is enhanced in the endometrium of human patients and Rhesus macaques with endometriosis. Their research also suggested the potential use of BLC as a biomarker for the disease. Analyses in the present thesis further showed elevated levels of TIMP-1 in the peritoneal fluid 14 days after endometriosis induction in mice. This cytokine is also linked to the pathophysiology of endometriosis, as it is secreted by endometriotic lesions in humans as well as in rats [Stilley et al., 2010]. The rat model used by Stilley et al. showed that the increased expression of TIMP-1 in the peritoneal fluid affects ovarian function and embryo development, leading to infertility.

Additionally, the present study showed lower expression levels of certain cytokines, including IL-2. IL-2 is secreted by activated T-cells and promotes T-cell growth and differentiation [Bachman & Oxenius, 2007]. Although IL-2 is typically expected to be elevated in the peritoneal fluid of endometriosis patients [Qiu et al, 2020], contradictory functions have been described, such as anti-inflammatory properties. IL-2 has been shown to suppress Th17 cells and IL-17 secretion [Bachman & Oxenius, 2007]. Thus, its downregulated expression correlates with the elevated IL-17 levels found in the present study.

In summary, the analysis of cytokine levels in the peritoneal fluid suggests that the increased proliferation rate of stromal cells and higher growth rate of lesions in the DT group were likely due to the stimulatory effects of the altered peritoneal milieu. The immune cell infiltration of

lesions assessed by means of immunohistochemistry showed higher numbers of CD3-positive lymphocytes in the DT group, suggesting an influence of the modified biochemical peritoneal conditions on the development of lesions in the DT group.

However, further limitations of this thesis must be mentioned. The statistical significance of the results may be limited by the small number of used mice, which was due to ethical considerations. Moreover, the growth of newly developing endometriotic lesions was only examined over a period of 28 days. Consequently, longer observation periods may have yielded different results.

7.3. Conclusion

The findings of the present study demonstrate that pre-existing endometriotic lesions promote the development of new lesions in the abdomen of mice. This is primarily due to an increased peritoneal inflammation, creating favorable conditions for the growth of new lesions. The higher growth rates of lesions were not associated with a relevant cellular exchange between the two types of lesions induced in this work (originating from either wild-type or transgenic mice). When translated to a clinical setting, these results suggest that patients with peritoneal endometriosis may be more susceptible to the establishment and growth of new endometriotic lesions, leading to the progression of the disease in a vicious cycle. Because endometriosis presents with non-specific symptoms and its management lacks highly specific diagnostic procedures, the diagnosis of the disease is frequently delayed for several years [Davenport et al., 2022; Mahini et al., 2023]. This highlights the importance of developing faster routines for diagnosing endometriosis, so that the eradication of lesions can be rapidly performed. Finding disease-specific molecular diagnostic markers in the eutopic endometrium of affected patients, or better yet in their plasma, would be a useful strategy to achieve this aim [Holzer et al., 2020; Zubrzycka et al., 2021]. Furthermore, the detection of specific molecules (e.g., CA-125) has been proven effective in diagnosing endometrial cancer. Similarly, discovering markers for endometriosis would significantly improve risk assessment and therapeutic management [Cuccu et al., 2023].

8. REFERENCES

1. **Abrao MS, Neme RM, Carvalho FM, Aldrighi JM, Pinotti JA. (2003)** Histological classification of endometriosis as a predictor of response to treatment. *Int J Gynaecol Obstet* 82:31-40.
2. **Agarwal SK, Chapron C, Giudice LC, Laufer MR, Leyland N, Missmer SA, Singh SS, Taylor HS. (2019)** Clinical diagnosis of endometriosis: a call to action. *Am J Obstet Gynecol* 220:354.e1-354.e12.
3. **Ahn SH, Edwards AK, Singh SS, Young SL, Lessey BA, Tayade C. (2015)** IL-17A contributes to the pathogenesis of endometriosis by triggering proinflammatory cytokines and angiogenic growth factors. *J Immunol* 195:2591-2600.
4. **Alarcon B, Berkhout B, Breitmeyer J, Terhorst C. (1988)** Assembly of the human T cell receptor-CD3 complex takes place in the endoplasmic reticulum and involves intermediary complexes between the CD3-gamma.delta.epsilon core and single T cell receptor alpha or beta chains. *J Biol Chem* 263:2953-2961.
5. **Allaire C, Bedaiwy MA, Yong PJ. (2023)** Diagnosis and management of endometriosis. *CMAJ* 195:E363-E371.
6. **Al-Talib A, Tulandi T. (2010)** Intestinal endometriosis. *Gyn Surg* 7:61-62.
7. **Andreoli CG, Genro VK, Souza CA, Michelon T, Bilibio JP, Scheffel C, Cunha-Filho JS. (2011)** T helper (Th) 1, Th2, and Th17 interleukin pathways in infertile patients with minimal/mild endometriosis. *Fertil Steril* 95:2477-2480.
8. **Bachmann MF, Oxenius A. (2007)** Interleukin 2: from immunostimulation to immunoregulation and back again. *EMBO Rep* 8:1142-1148.
9. **Becker CM, Wright RD, Satchi-Fainaro R, Funakoshi T, Folkman J, Kung AL, D'Amato RJ. (2006)** A novel noninvasive model of endometriosis for monitoring the efficacy of antiangiogenic therapy. *Am J Pathol* 168:2074-2084.
10. **Becker CM, Bokor A, Heikinheimo O, Horne A, Jansen F, Kiesel L, King K, Kvaskoff M, Nap A, Petersen K, Saridogan E, Tomassetti C, van Hanegem N, Vulliemoz N, Vermeulen N, ESHRE Endometriosis Guideline Group. (2022)** ESHRE guideline: endometriosis. *Hum Reprod Open* 2022:hoac009.
11. **Beste MT, Pfäffle-Doyle N, Prentice EA, Morris SN, Lauffenburger DA, Isaacson KB, Griffith LG. (2014)** Molecular network analysis of endometriosis reveals a role for c-Jun-regulated macrophage activation. *Sci Transl Med* 6:222ra16.

12. **Braundmeier AG, Fazleabas AT. (2009)** The non-human primate model of endometriosis: research and implications for fecundity. *Mol Hum Reprod* 15:577-586.
13. **Breschi A, Gingeras TR, Guigó R. (2017)** Comparative transcriptomics in human and mouse. *Nat Rev Genet* 18:425-440.
14. **Brosens I, Brosens JJ, Benagiano G. (2012)** The eutopic endometrium in endometriosis: are the changes of clinical significance? *Reprod Biomed Online* 24:496-502.
15. **Bryda EC. (2013)** The Mighty Mouse: the impact of rodents on advances in biomedical research. *Mo Med* 110:207-211.
16. **Bulun SE, Yilmaz BD, Sison C, Miyazaki K, Bernardi L, Liu S, Kohlmeier A, Yin P, Milad M, Wei J. (2019)** Endometriosis. *Endocr Rev* 40:1048-1079.
17. **Bulun, SE. (2022)** Endometriosis caused by retrograde menstruation: now demonstrated by DNA evidence. *Fertil Steril* 118:535-536.
18. **Burns KA, Pearson AM, Slack JL, Por ED, Scribner AN, Eti NA, Burney RO. (2022)** Endometriosis in the mouse: challenges and progress toward a 'best fit' murine model. *Front Physiol* 12:806574.
19. **Ceccaroni M, Bounous VE, Clarizia R, Mautone D, Mabrouk M. (2019)** Recurrent endometriosis: a battle against an unknown enemy. *Eur J Contracept Reprod Health Care* 24:464-474.
20. **Chantalat E, Valera MC, Vaysse C, Noirrit E, Rusidze M, Weyl A, Vergriete K, Buscail E, Lluel P, Fontaine C, Arnal JF, Lenfant F. (2020)** Estrogen receptors and endometriosis. *Int J Mol Sci* 21:2815.
21. **Christ JP, Yu O, Schulze-Rath R, Grafton J, Hansen K, Reed SD. (2021)** Incidence, prevalence, and trends in endometriosis diagnosis: a United States population-based study from 2006 to 2015. *Am J Obstet Gynecol* 225:500.e1-500.e9.
22. **Coccia ME, Nardone L, Rizzello F. (2022)** Endometriosis and infertility: a long-life approach to preserve reproductive integrity. *Int J Environ Res Public Health* 19:6162.
23. **Cora MC, Kooistra L, Travlos G. (2015)** Vaginal cytology of the laboratory rat and mouse: review and criteria for the staging of the estrous cycle using stained vaginal smears. *Toxicol Pathol* 43:776-793.
24. **Cuccu I, D'Oria O, Sgamba L, De Angelis E, Golia D'Augè T, Turetta C, Di Dio C, Scudo M, Bogani G, Di Donato V, Palaia I, Perniola G, Tomao F, Muzii L, Giannini A. (2023)** Role of genomic and molecular biology in the modulation of the treatment of endometrial cancer: narrative review and perspectives. *Healthcare (Basel)* 11:571.

25. **Culley L, Law C, Hudson N, Denny E, Mitchell H, Baumgarten M, Raine-Fenning N. (2013)** The social and psychological impact of endometriosis on women's lives: a critical narrative review. *Hum Reprod Update* 19:625-639.
26. **Davenport S, Smith D, Green DJ. (2022)** Barriers to a timely diagnosis of endometriosis: a qualitative systematic review. *Obstet Gynecol* 5:10-97.
27. **Dorning A, Dhami P, Panir K, Hogg C, Park E, Ferguson GD, Hargrove D, Karras J, Horne AW, Greaves E. (2021)** Bioluminescent imaging in induced mouse models of endometriosis reveals differences in four model variations. *Dis Model Mech* 14:dmm049070.
28. **Fan D, Wang X, Shi ZX, Jiang YT, Zheng BH, Xu L, Zhou ST. (2023)** Understanding endometriosis from an immunomicroenvironmental perspective. *Chin Med J* 136:1897-1909.
29. **Ferrero H, Buigues A, Martínez J, Simón C, Pellicer A, Gómez R. (2017)** A novel homologous model for noninvasive monitoring of endometriosis progression. *Biol Reprod* 96:302-312.
30. **Franasiak JM, Burns KA, Slayden O, Yuan L, Fritz MA, Korach KS, Lessey BA, Young SL. (2015)** Endometrial CXCL13 expression is cycle regulated in humans and aberrantly expressed in humans and Rhesus macaques with endometriosis. *Reprod Sci* 22:442-451.
31. **Gao X, Outley J, Botteman M, Spalding J, Simon JA, Pashos CL. (2006)** Economic burden of endometriosis. *Fertil Steril* 86:1561-1572.
32. **Giudice LC, Kao LC. (2004)** Endometriosis. *Lancet* 364:1789-1799.
33. **Gogacz M, Winkler I, Bojarska-Junak A, Tabarkiewicz J, Semczuk A, Rechberger T, Adamiak A. (2016)** Increased percentage of Th17 cells in peritoneal fluid is associated with severity of endometriosis. *J Reprod Immunol* 117:39-44.
34. **Grandi G, Barra F, Ferrero S, Sileo FG, Bertucci E, Napolitano A, Facchinetti F. (2019)** Hormonal contraception in women with endometriosis: a systematic review. *Eur J Contracept Reprod Health Care* 24:61-70.
35. **Greaves E, Cousins FL, Murray A, Esnal-Zufiaurre A, Fassbender A, Horne AW, Saunders PT. (2014)** A novel mouse model of endometriosis mimics human phenotype and reveals insights into the inflammatory contribution of shed endometrium. *Am J Pathol* 184:1930-1939.
36. **Gruenwald P. (1942)** Origin of endometriosis from the mesenchyme of the celomic walls. *Am J Obstet Gynecol* 44:470-474.

37. **Grümmer R, Schwarzer F, Bainczyk K, Hess-Stumpp H, Regidor PA, Schindler AE, Winterhager E. (2001)** Peritoneal endometriosis: validation of an in-vivo model. *Hum Reprod* 16:1736-1743.
38. **Halme J, Hammond MG, Hulka JF, Raj SG, Talbert LM. (1984)** Retrograde menstruation in healthy women and in patients with endometriosis. *Obstet Gynecol* 64:151-154.
39. **Harada T, Iwabe T, Terakawa N. (2001)** Role of cytokines in endometriosis. *Fertil Steril* 76:1-10.
40. **Hassani M, Koenderman L. (2018)** Immunological and hematological effects of IL-5 (Rα)-targeted therapy: an overview. *Allergy* 73:1979-1988.
41. **Holzer I, Machado Weber A, Marshall A, Freis A, Jauckus J, Strowitzki T, Germeyer A. (2020)** GRN, NOTCH3, FN1, and PINK1 expression in eutopic endometrium–potential biomarkers in the detection of endometriosis–a pilot study. *J Assist Reprod Genet* 37:2723-2732.
42. **Hornung D, Dohrn K, Sotlar K, Greb RR, Wallwiener D, Kiesel L, Taylor RN. (2000)** Localization in tissues and secretion of eotaxin by cells from normal endometrium and endometriosis. *J Clin Endocrinol Metab* 85:2604-2608.
43. **Hsu AL, Khachikyan I, Stratton P. (2010)** Invasive and noninvasive methods for the diagnosis of endometriosis. *Clin Obstet Gynecol* 53:413-419.
44. **Imperiale L, Nisolle M, Noël JC, Fastrez M. (2023)** Three types of endometriosis: pathogenesis, diagnosis and treatment. State of the Art. *J Clin Med* 12:994.
45. **Izumi G, Koga K, Takamura M, Makabe T, Satake E, Takeuchi A, Taguchi A, Urata Y, Fujii T, Osuga Y. (2018)** Involvement of immune cells in the pathogenesis of endometriosis. *J Obstet Gynaecol Res* 44:191-198.
46. **Jacobson TZ, Duffy JM, Barlow D, Farquhar C, Koninckx PR, Olive D. (2010)** Laparoscopic surgery for subfertility associated with endometriosis. *Cochrane Database Syst Rev* CD001398.
47. **Jiang I, Yong PJ, Allaire C, Bedaiwy MA. (2021)** Intricate connections between the microbiota and endometriosis. *Int J Mol Sci* 22:5644.
48. **Jørgensen H, Hill AS, Beste MT, Kumar MP, Chiswick E, Fedorcsak P, Isaacson KB, Lauffenburger DA, Griffith LG, Qvigstad E. (2017)** Peritoneal fluid cytokines related to endometriosis in patients evaluated for infertility. *Fertil Steril* 107:1191-1199.e2.

49. Kalu E, Sumar N, Giannopoulos T, Patel P, Croucher C, Sherriff E, Bansal A. (2007) Cytokine profiles in serum and peritoneal fluid from infertile women with and without endometriosis. *J Obstet Gynaecol Res* 33:490-495.

50. Körbel C, Menger MD, Laschke MW. (2010) Size and spatial orientation of uterine tissue transplants on the peritoneum crucially determine the growth and cyst formation of endometriosis-like lesions in mice. *Hum Reprod* 25:2551-2558.

51. Kunisch E, Fuhrmann R, Roth A, Winter R, Lungershausen W, Kinne RW. (2004) Macrophage specificity of three anti-CD68 monoclonal antibodies (KP1, EBM11, and PGM1) widely used for immunohistochemistry and flow cytometry. *Ann Rheum Dis* 63:774-784.

52. Laschke MW, Körbel C, Rudzitis-Auth J, Gashaw I, Reinhardt M, Hauff P, Zollner TM, Menger MD. (2010) High-resolution ultrasound imaging: a novel technique for the noninvasive in vivo analysis of endometriotic lesion and cyst formation in small animal models. *Am J Pathol* 176:585-593.

53. Lee SY, Koo YJ, Lee DH. (2021) Classification of endometriosis. *J Yeungnam Med Sci* 38:10-18.

54. Liu H, Lang JH. (2011) Is abnormal eutopic endometrium the cause of endometriosis? The role of eutopic endometrium in pathogenesis of endometriosis. *Med Sci Monit* 17:RA92-99.

55. Mahini SM, Younesi M, Mortazavi G, Samare-Najaf M, Azadbakht MK, Jamali N. (2023) Non-invasive diagnosis of endometriosis: immunologic and genetic markers. *Clin Chim Acta* 538:70-86.

56. Maruyama T. (2022) A revised stem cell theory for the pathogenesis of endometriosis. *J Pers Med* 12:216.

57. May KE, Villar J, Kirtley S, Kennedy SH, Becker CM. (2011) Endometrial alterations in endometriosis: a systematic review of putative biomarkers. *Hum Reprod Update* 17:637-653.

58. Mihai IT, Rudzitis-Auth J, Menger MD, Laschke MW. (2023) The presence of pre-existing endometriotic lesions promotes the growth of new lesions in the peritoneal cavity. *Int J Mol Sci* 24:13858.

59. Milewski Ł, Dziunycz P, Barcz E, Radomski D, Roszkowski PI, Korczak-Kowalska G, Kamiński P, Malejczyk J. (2011) Increased levels of human neutrophil peptides 1, 2, and 3 in peritoneal fluid of patients with endometriosis: association with neutrophils, T cells and IL-8. *J Reprod Immunol* 91:64-70.

60. **Mok-Lin EY, Wolfberg A, Hollinquist H, Laufer MR. (2010)** Endometriosis in a patient with Mayer-Rokitansky-Küster-Hauser syndrome and complete uterine agenesis: evidence to support the theory of coelomic metaplasia. *J Pediatr Adolesc Gynecol* 23:e35-e37.
61. **Monsanto SP, Edwards AK, Zhou J, Nagarkatti P, Nagarkatti M, Young SL, Tayade C. (2016)** Surgical removal of endometriotic lesions alters local and systemic proinflammatory cytokines in endometriosis patients. *Fertil Steril* 105:968-977.
62. **Moradi Y, Shams-Beyranvand M, Khateri S, Gharahjeh S, Tehrani S, Varse F, Tiyuri A, Najmi Z. (2021)** A systematic review on the prevalence of endometriosis in women. *Indian J Med Res* 154:446-454.
63. **Morotti M, Vincent K, Brawn J, Zondervan KT, Becker CM. (2014)** Peripheral changes in endometriosis-associated pain. *Hum Reprod Update* 20:717-736.
64. **Mounsey AL, Wilgus A, Slawson DC. (2006)** Diagnosis and management of endometriosis. *Am Fam Physician* 74:594-600.
65. **Nauseef WM, Olsson I, Arnljots K. (1988)** Biosynthesis and processing of myeloperoxidase — A marker for myeloid cell differentiation. *Eur J Haematol* 40:97-110.
66. **Nisenblat V, Bossuyt PM, Farquhar C, Johnson N, Hull ML. (2016)** Imaging modalities for the non-invasive diagnosis of endometriosis. *Cochrane Database Syst Rev* 2:CD009591.
67. **Nisolle M, Donnez J. (1997)** Peritoneal endometriosis, ovarian endometriosis, and adenomyotic nodules of the rectovaginal septum are three different entities. *Fertil Steril* 68:585-596.
68. **Pantier LK, Li J, Christian CA. (2019)** Estrous cycle monitoring in mice with rapid data visualization and analysis. *Bio Protoc* 9:e3354.
69. **Parasar P, Ozcan P, Terry KL. (2017)** Endometriosis: epidemiology, diagnosis and clinical management. *Curr Obstet Gynecol Rep* 6:34-41.
70. **Pašalić E, Tambuwala MM, Hromić-Jahjefendić A. (2023)** Endometriosis: classification, pathophysiology, and treatment options. *Pathol Res Pract* 251:154847.
71. **Practice Committee of the American Society for Reproductive Medicine. (2012)** Endometriosis and infertility: a committee opinion. *Fertil Steril* 98:591-598.
72. **Pundir J, Omanwa K, Kovoor E, Pundir V, Lancaster G, Barton-Smith P. (2017)** Laparoscopic excision versus ablation for endometriosis-associated pain: an updated systematic review and meta-analysis. *J Minim Invasive Gynecol* 24:747-756.
73. **Qiu XM, Lai ZZ, Ha SY, Yang HL, Liu LB, Wang Y, Shi JW, Ruan LY, Ye JF, Wu JN, Fu Q, Yi XF, Chang KK, Li MQ. (2020)** IL-2 and IL-27 synergistically promote growth

and invasion of endometriotic stromal cells by maintaining the balance of IFN-γ and IL-10 in endometriosis. *Reproduction* 159:251-260.

74. **Rakhila H, Al-Akoum M, Bergeron ME, Leboeuf M, Lemyre M, Akoum A, Pouliot M. (2016)** Promotion of angiogenesis and proliferation cytokines patterns in peritoneal fluid from women with endometriosis. *J Reprod Immunol* 116:1-6.
75. **Riccio LDGC, Santulli P, Marcellin L, Abrão MS, Batteux F, Chapron C. (2018)** Immunology of endometriosis. *Best Pract Res Clin Obstet Gynaecol* 50:39-49.
76. **Rudzitis-Auth J, Christoffel A, Menger MD, Laschke MW. (2021)** Targeting sphingosine kinase-1 with the low MW inhibitor SKI-5C suppresses the development of endometriotic lesions in mice. *Br J Pharmacol* 178:4104-4118.
77. **Rudzitis-Auth J, Becker M, Scheuer C, Menger MD, Laschke MW. (2022a)** Indole-3-carbinol inhibits the growth of endometriotic lesions by suppression of microvascular network formation. *Nutrients* 14:4940.
78. **Rudzitis-Auth J, Huwer SI, Scheuer C, Menger MD, Laschke MW. (2022b)** The ischemic time window of ectopic endometrial tissue crucially determines its ability to develop into endometriotic lesions. *Sci Rep* 12:5625.
79. **Sampson JA. (1927)** Peritoneal endometriosis due to menstrual dissemination of endometrial tissues into the peritoneal cavity. *Am J Obstet Gynecol* 14:422-469.
80. **Sarria-Santamera A, Orazumbekova B, Terzic M, Issanov A, Chaowen C, Asúnsolo-del-Barco A. (2021)** Systematic review and meta-analysis of incidence and prevalence of endometriosis. *Healthcare* 9:29.
81. **Schmitz T, Hoffmann V, Olliges E, Bobinger A, Popovici R, Nößner E, Meissner K. (2021)** Reduced frequency of perforin-positive CD8+ T cells in menstrual effluent of endometriosis patients. *J Reprod Immunol* 148:103424.
82. **Scholzen T, Gerdes J. (2000)** The Ki-67 protein: from the known and the unknown. *J Cell Physiol* 182:311-322.
83. **Sheikh AY, Lin SA, Cao F, Cao Y, van der Bogt KE, Chu P, Chang CP, Contag CH, Robbins RC, Wu JC. (2007)** Molecular imaging of bone marrow mononuclear cell homing and engraftment in ischemic myocardium. *Stem Cells* 25:2677-2684.
84. **Shi JL, Zheng ZM, Chen M, Shen HH, Li MQ, Shao J. (2022)** IL-17: an important pathogenic factor in endometriosis. *Int J Med Sci* 19:769-778.
85. **Siegenthaler F, Knabben L, Mohr S, Nirgianakis K, Imboden S, Mueller MD. (2020)** Visualization of endometriosis with laparoscopy and near-infrared optics with indocyanine green. *Acta Obstet Gynecol Scand* 99:591-597.

86. Signorile PG, Viceconte R, Baldi A. (2022) New insights in pathogenesis of endometriosis. *Front Med (Lausanne)* 9:879015.

87. Simoens S, Hummelshoj L, D'Hooghe T. (2007) Endometriosis: cost estimates and methodological perspective. *Hum Reprod Update* 13:395-404.

88. Sisnett DJ, Zutautas KB, Miller JE, Lingegowda H, Ahn SH, McCallion A, Bougie O, Lessey BA, Tayade C. (2023) The dysregulated IL-23/T_H17 axis in endometriosis pathophysiology. *bioRxiv* [Preprint]. 08 December, 2023. [accessed on 04 February, 2024]. Available from https://doi.org/10.1101/2023.12.07.570652.

89. Stilley JA, Birt JA, Nagel SC, Sutovsky M, Sutovsky P, Sharpe-Timms KL. (2010) Neutralizing TIMP1 restores fecundity in a rat model of endometriosis and treating control rats with TIMP1 causes anomalies in ovarian function and embryo development. *Biol Reprod* 83:185-194.

90. Surrey E, Soliman AM, Trenz H, Blauer-Peterson C, Sluis A. (2020) Impact of endometriosis diagnostic delays on healthcare resource utilization and costs. *Adv Ther* 37:1087-1099.

91. Surrey ES. (2022) GnRH agonists in the treatment of symptomatic endometriosis: a review. *F S Rep* 4:40-45.

92. Symons LK, Miller JE, Kay VR, Marks RM, Liblik K, Koti M, Tayade C. (2018) The immunopathophysiology of endometriosis. *Trends Mol Med* 24:748-762.

93. Takamura M, Koga K, Izumi G, Urata Y, Nagai M, Hasegawa A, Harada M, Hirata T, Hirota Y, Wada-Hiraike O, Fujii T, Osuga Y. (2016) Neutrophil depletion reduces endometriotic lesion formation in mice*. Am J Reprod Immunol* 76:193-198.

94. Tal A, Tal R, Pluchino N, Taylor HS. (2019) Endometrial cells contribute to preexisting endometriosis lesions in a mouse model of retrograde menstruation. *Biol Reprod* 100:1453-1460.

95. Tampaki EC, Tampakis A, Kontzoglou K, Kouraklis G. (2017) Somatic stem cells and their dysfunction in endometriosis. *Front Surg* 4:37.

96. Tosti C, Pinzauti S, Santulli P, Chapron C, Petraglia F. (2015) Pathogenetic mechanisms of deep infiltrating endometriosis. *Reprod Sci* 22:1053-1059.

97. Tuttlies F, Keckstein J, Ulrich U, Possover M, Schweppe KW, Wustlich M, Buchweitz O, Greb R, Kandolf O, Mangold R, Masetti W, Neis K, Rauter G, Reeka N, Richter O, Schindler AE, Sillem M, Terruhn V, Tinneberg HR. (2005) ENZIAN-Score, eine Klassifikation der tief infiltrierenden Endometriose. *Zent Gynakol* 127:275-281.

98. **Vallvé-Juanico J, Houshdaran S, Giudice LC. (2019)** The endometrial immune environment of women with endometriosis. *Hum Reprod Update* 25:564-591.

99. **Vodolazkaia A, El-Aalamat Y, Popovic D, Mihalyi A, Bossuyt X, Kyama CM, Fassbender A, Bokor A, Schols D, Huskens D, Meuleman C, Peeraer K, Tomassetti C, Gevaert O, Waelkens E, Kasran A, De Moor B, D'Hooghe TM. (2012)** Evaluation of a panel of 28 biomarkers for the non-invasive diagnosis of endometriosis. *Hum Reprod* 27:2698-2711.

100. **Whitaker LHR, Saraswat L, Horne AW. (2022)** Combination GnRH antagonists for endometriosis: balancing efficacy with side effects. *Cell Rep Med* 3:100748.

101. **Wibisono H, Nakamura K, Taniguchi F, Seno M, Morimoto K, Yoshimura Y, Harada T. (2022)** Tracing location by applying Emerald luciferase in an early phase of murine endometriotic lesion formation. *Exp Anim* 71:184-192.

102. **Wu J, Xie H, Yao S, Liang Y. (2017)** Macrophage and nerve interaction in endometriosis. *J Neuroinflamm* 14:53-59.

103. **Yip KS, Suvorov A, Connerney J, Lodato NJ, Waxman DJ. (2013)** Changes in mouse uterine transcriptome in estrus and proestrus. *Biol Reprod* 89:13.

104. **Zito G, Luppi S, Giolo E, Martinelli M, Venturin I, Di Lorenzo G, Ricci G. (2014)** Medical treatments for endometriosis-associated pelvic pain. *Biomed Res Int* 2014:191967.

105. **Zubrzycka A, Migdalska-Sęk M, Jędrzejczyk S, Brzeziańska-Lasota E. (2021)** Circulating miRNAs related to Epithelial-Mesenchymal Transitions (EMT) as the new molecular markers in endometriosis. *Curr Issues Mol Biol* 43:900-916.

9. ACKNOWLEDGEMENTS

I would like to thank all people that guided and helped me throughout my thesis.

My gratitude goes to Prof. Dr. Michael D. Menger for the opportunity of graduating my doctorate at the Institute for Clinical and Experimental Surgery at Saarland University. Prof. Dr. Matthias Laschke I would like to thank for granting me the topic of this dissertation and for offering me his continuous support along the entire work process, while also giving me helpful criticism. Special thanks go to Dr. Jeannette Rudzitis-Auth, who taught me all I needed to know to complete the experiments for this research, meeting my needs with great patience and professionalism and advising me on all issues that I confronted.

I would also like to thank all the colleagues working at the Institute for Clinical and Experimental Surgery, making me feel welcome in the pleasant environment that they create, showing me also eagerness to help and assist me as I needed. Many thanks go to Janine Becker, Caroline Bickelmann, Sandra Hans and Ruth Nickels, who helped me with completing all laboratory analyses, such as the immunohistochemical sections, flow cytometry and cytokine assays. In addition, I would like to thank Elisabeth Gluding and all other laboratory animal keepers.

Special thanks go to my family and friends, who always supported and motivated me throughout this great experience.

10. CURRICULUM VITAE

Aus datenschutzrechtlichen Gründen wird der Lebenslauf in der elektronischen Fassung der Dissertation nicht veröffentlicht.

Tag der Promotion: 18. August 2025
Dekan: Univ.-Prof. Dr. med. dent. Matthias Hannig
Berichterstatter: Prof. Dr. med. Matthias Laschke
Prof. Dr. med. Erich Solomayer

11. PUBLICATION

The results of this thesis are included in the following original publication:

Mihai IT, Rudzitis-Auth J, Menger MD, Laschke MW. (2023) The presence of pre-existing endometriotic lesions promotes the growth of new lesions in the peritoneal cavity. *Int J Mol Sci* 24:13858.